Report No. FHWA-KS-02-9
FINAL REPORT

EVALUATION OF CORROSION RESISTANCE OF MICROALLOYED REINFORCING STEEL

Javier Balma
David Darwin
JoAnn P. Browning
Carl E. Locke, Jr.
University of Kansas

FEBRUARY 2004

KANSAS DEPARTMENT OF TRANSPORTATION

Division of Operations
Bureau of Materials and Research

1 Report No. FHWA-KS-02-9	2 Government Accession No.	3 Recipient Catalog No.	
4 Title and Subtitle EVALUATION OF CORROSION RESISTANCE OF MICROALLOYED REINFORCING STEEL		**5 Report Date** February 2004	
		6 Performing Organization Code	
7 Author(s) Javier Balma, David Darwin, JoAnn P. Browning and Carl E. Locke, Jr.		**8 Performing Organization Report No.**	
9 Performing Organization Name and Address The University of Kansas 1530 West 15th Street Lawrence, Kansas 66045		**10 Work Unit No. (TRAIS)**	
		11 Contract or Grant No. C1131/C1281	
12 Sponsoring Agency Name and Address Kansas Department of Transportation Bureau of Materials and Research, Research Unit 2300 Southwest Van Buren Street Topeka, Kansas 66611-1195		**13 Type of Report and Period Covered** Final Report January 1999 – December 2002	
		14 Sponsoring Agency Code RE-0223-01/RE-0298-01	

15 Supplementary Notes
For more information write to address in block 9.

16 Abstract

The corrosion resistance of three microalloyed steels and two conventional reinforcing steels in concrete was evaluated. The microalloyed steels contain concentrations of chromium, copper, and phosphorus that, while low, are significantly higher than used in conventional reinforcing steel. Two of the microalloyed steels contain amounts of phosphorus that exceed the amounts allowed in ASTM specifications (ASTM A 615), while the other microalloyed steel has normal amounts of phosphorus. One of the conventional steels and the three microalloyed steels are heat treated by the Thermex process, which includes quenching and tempering of the steel immediately after rolling, while the other conventional steel is hot-rolled. The study was undertaken because earlier tests on similar steels indicated that the Thermex-treated, microalloyed steel corrodes at only one-half the rate of conventional reinforcing steel. The relative corrosion rate dropped to one-tenth if both steels were epoxy-coated. In the current study, the reinforcing steels were tested using two rapid evaluation tests, the corrosion potential and corrosion macrocell tests, and three bench-scale tests, the Southern Exposure, cracked beam, and ASTM G 109 tests. The corrosion potential, corrosion rate, and mat-to-mat resistance are used to evaluate the steel. Tension and bending tests were performed to evaluate the effect of the microalloying and heat treatment on the mechanical properties of the reinforcing steel.

Results show that the corrosion potential of the five steels is approximately the same, indicating that they have a similar tendency to corrode. The results from the rapid macrocell test showed that the five steels had similar corrosion rates, with no improved behavior for the microalloyed steels. The microalloyed steel with regular phosphorus content (CRT) exhibited consistently lower corrosion losses than conventional steel in the bench-scale tests. Although CRT appears to be much more corrosion resistant than conventional steel in the G 109 tests (64 percent less total corrosion loss after 70 weeks), its overall performance does not show such an advantage. In the cracked beam test after 70 weeks, it had only 4 percent less corrosion loss than conventional steel, which indicates that in cracked concrete the two steels behave in a similar manner. In the Southern Exposure test, CRT steel had an 11 percent lower corrosion loss than conventional steel after the same period. This improved behavior is not enough to use the steel without an epoxy coating or to justify continued research on the steel as a superior epoxy-coated material. The mechanical properties of the microalloyed steels were similar to those of conventional steel, indicating that the increased phosphorus content did not affect the mechanical properties.

17 Key Words Corrosion, Concrete, Cracking, Epoxy, Microalloyed Steel, Reinforcing Steel and Testing		**18 Distribution Statement** No restrictions. This document is available to the public through the National Technical Information Service, Springfield, Virginia 22161	
19 Security Classification (of this report) Unclassified	**20 Security Classification (of this page)** Unclassified	**21 No. of pages** 177	**22 Price**

Form DOT F 1700.7 (8-72)

EVALUATION OF CORROSION RESISTANCE OF MICROALLOYED REINFORCING STEEL

Final Report

Prepared by

Javier Balma
David Darwin
JoAnn P. Browning
Carl E. Locke, Jr.

all with
The University of Kansas

NOTICE

The authors and the state of Kansas do not endorse products or manufacturers. Trade and manufacturers names appear herein solely because they are considered essential to the object of this report.

This information is available in alternative accessible formats. To obtain an alternative format, contact the Office of Transportation Information, Kansas Department of Transportation, 915 SW Harrison Street, Room 754, Topeka, Kansas 66612-1568 or phone (785) 296-3585 (Voice) (TDD).

DISCLAIMER

The contents of this report reflect the views of the authors who are responsible for the facts and accuracy of the data presented herein. The contents do not necessarily reflect the views or the policies of the state of Kansas. This report does not constitute a standard, specification or regulation.

ABSTRACT

The corrosion resistance of three microalloyed steels and two conventional reinforcing steels in concrete was evaluated. The microalloyed steels contain concentrations of chromium, copper, and phosphorus that, while low, are significantly higher than used in conventional reinforcing steel. Two of the microalloyed steels contain amounts of phosphorus that exceed the amounts allowed in ASTM specifications (ASTM A 615), while the other microalloyed steel has normal amounts of phosphorus. One of the conventional steels and the three microalloyed steels are heat treated by the Thermex process, which includes quenching and tempering of the steel immediately after rolling, while the other conventional steel is hot-rolled.   The study was undertaken because earlier tests on similar steels indicated that the Thermex-treated, microalloyed steel corrodes at only one-half the rate of conventional reinforcing steel. The relative corrosion rate dropped to one-tenth if both steels were epoxy-coated. In the current study, the reinforcing steels were tested using two rapid evaluation tests; the corrosion potential and corrosion macrocell tests, and three bench-scale tests; the Southern Exposure, cracked beam, and ASTM G 109 tests. The corrosion potential, corrosion rate, and mat-to-mat resistance are used to evaluate the steel. Tension and bending tests were performed to evaluate the effect of the microalloying and heat treatment on the mechanical properties of the reinforcing steel.

Results show that the corrosion potential of the five steels is approximately the same, indicating that they have a similar tendency to corrode. The results from the rapid macrocell test showed that the five steels had similar corrosion rates, with no improved

behavior for the microalloyed steels. The microalloyed steel with regular phosphorus content (CRT) exhibited consistently lower corrosion losses than conventional steel in the bench-scale tests. Although CRT appears to be much more corrosion resistant than conventional steel in the G 109 tests (64 percent less total corrosion loss after 70 weeks), its overall performance does not show such an advantage. In the cracked beam test after 70 weeks, it had only 4 percent less corrosion loss than conventional steel, which indicates that in cracked concrete the two steels behave in a similar manner. In the Southern Exposure test, CRT steel had an 11 percent lower corrosion loss than conventional steel after the same period. This improved behavior is not enough to use the steel without an epoxy coating or to justify continued research on the steel as a superior epoxy-coated material. The mechanical properties of the microalloyed steels were similar to those of conventional steel, indicating that the increased phosphorus content did not affect the mechanical properties.

ACKNOWLEDGEMENTS

TABLE OF CONTENTS

LIST OF TABLES

LIST OF FIGURES

Chapter 1

Introduction

1.1   General

One of the major durability problems in reinforced concrete structures is the corrosion of the

reinforcing steel. According to the Federal Highway Administration (FHWA), approximately 30

percent of the nation's bridges are classified as either structurally or functionally deficient

(FHWA 1999). It is estimated that it will cost an average $10.6 billion a year for 20 years to

eliminate the existing bridge investment backlog and correct bridge deficiencies that are likely to

develop over this period. If the bridge investment backlog is maintained at its current level, it

will take an average $5.8 billion a year for that same period to selectively correct existing

deficiencies and other deficiencies that will develop with time.

Due to the bare pavement policies implemented during the 1950s, deicing salts such as

sodium chloride and calcium chloride are used on highways and bridges to keep them free of ice

and snow. These chlorides can penetrate the concrete and attack the reinforcing steel, causing

corrosion. Bridge decks are most likely to be damaged, but other elements, such as beams and

piers, can also be affected due to runoff. Structures in marine environments are also subjected to

chloride-induced corrosion. Corrosion causes cracking and spalling of concrete due to the

increased volume of corrosion products compared to the original steel. Loss of bond between the

reinforcing steel and the concrete and loss of steel area also reduce the strength of the member.

Several methods to protect reinforcing steel from corrosion have been developed over the

years. These methods include barriers that prevent chlorides from reaching the steel (overlays,

sealers), electrochemical methods (cathodic protection), corrosion inhibitors in the concrete, and

alternative reinforcing steels, such as stainless steel or epoxy-coated reinforcing bars. This study focuses on the evaluation of the corrosion-resistant properties of three different microalloyed steels.

Tata Steel Company in India originally developed a microalloyed steel with mechanical properties similar to those of conventional steel and with corrosion resistance that was claimed by the original developers to be three to five times better than conventional steel (Tata 1991). The alloying process is carried out "to affect the electrochemical behavior in such a way that either the corrosion potential increases or the critical current density decreases, so that the on-set of anodic reaction gets lowered" (Tata 1991). These microalloyed steels have a carbon equivalent of 0.30 to 0.45 percent, and the alloys contain concentrations of chromium, copper and phosphorus that, while low, are significantly higher than used in conventional reinforcing steel. According to Tata (1991), the copper reacts with chlorides on the steel surface to form a layer of $CuCl_2 \cdot 3\,Cu(OH)_2$ that has low solubility and retards the corrosion process. Phosphorus oxides act as inhibitors and also slow the corrosion process. Chromium results in the formation of a spinel oxide layer ($FeO \cdot Cr_2O_3$) that is a poor conductor of electrons. Some of the steel is also heat treated by the Tempcore or Thermex process (trade names), which involves quenching and tempering of the steel immediately after rolling. This process places the exterior of the bars in compression, reducing microcracks on the surface of the steel.

Accelerated corrosion tests were conducted by Tata Steel to select the best chemistry for the corrosion resistant steel (CRS). The accelerated corrosion tests on bare steel included: salt spray, alternate immersion in salt water, placement in a sulfur dioxide chamber, and potentiodynamic tests. Atmospheric corrosion tests were also conducted for periods of two months to two years. Tests on bars embedded in concrete consisted of exposing the concrete

blocks in a saline solution to 60 cycles of wetting and drying. Each cycle consisted of 24 hours of immersion of the concrete block in a saline solution, then drying for 48 hours at room temperature, followed by drying at $60^{o}C$ ($140^{o}F$) in an air circulation chamber for 48 hours. After 50 cycles, the concrete blocks containing CRS bars were intact, while concrete blocks containing conventional steel had disintegrated due to volume expansion of the corrosion products. Salt spray tests conducted for 720 hours resulted in a severely pitted surface for conventional steel, while CRS bars showed a smooth surface. Bars rolled using the Thermex process were more corrosion resistant than the bars rolled using conventional methods.

Similar microalloyed steels, provided by Gerdau AmeriSteel (formerly Florida Steel Corporation) were evaluated at the University of Kansas (Senecal et al. 1995, Smith et al. 1995, Schwensen et al. 1995, Darwin 1995). Four types of steel, hot-rolled conventional, Thermex-treated conventional, hot-rolled microalloyed, and Thermex- treated microalloyed steel, were evaluated. Corrosion potential, macrocell, Southern Exposure and cracked beam tests were performed. The Southern Exposure and cracked beam tests (bench-scale tests) lasted for 48 weeks. The corrosion potential and macrocell tests are described in Section 2.3 and the Southern Exposure and cracked beam tests are described in Section 2.4.

In general, the Thermex-treated microalloyed steel had a macrocell corrosion rate equal to about one-half that of conventional steels in both the rapid macrocell and the Southern Exposure tests. The hot-rolled microalloyed steel showed higher corrosion rates than conventional steels in the bench-scale tests, but exhibited half the corrosion rate of conventional steel in the rapid macrocell test. The Thermex-treated conventional steel showed improved corrosion resistance compared to the hot-rolled conventional steel. All four types of steel showed similar corrosion potentials when exposed to the same concentrations of NaCl. Epoxy-coated

3

Thermex-treated microalloyed steel performed particularly better when compared to conventional epoxy-coated steel (corroding at only about 10 percent of the rate). Based on these observations, a recommendation was made to continue development of the new steel to be used as a superior epoxy-coated reinforcing steel. In addition, a recommendation was made to extend the testing period for the bench-scale tests to two years to better evaluate the corrosion behavior as affected by the deposition of corrosion products.

In the current study, two rapid evaluation tests, the corrosion potential and macrocell tests, and three bench-scale tests, the Southern Exposure (SE), cracked beam (CB), and ASTM G 109 tests, described in Chapter 2, are used to evaluate new microalloyed reinforcing steels. Tension tests and bend tests are performed to determine the mechanical properties and the ductility of the steels. The balance of this chapter provides background for the tests performed in this study.

1.2   Corrosion of Steel in Concrete

Metals are usually reduced from chemical compounds (minerals, ores), and a certain amount of energy is needed for this process. The corrosion process returns the metals to their original chemical compounds, releasing the same amount of energy, although at a different rate. Jones (1996) defines corrosion as "the destructive result of chemical reaction between a metal or metal alloy and its environment."

Steel corrosion products (rust) have a greater volume, three to five times more, than the original metal. This produces internal compressive stresses at the steel/mortar interface that produce tension in the surrounding material and results in cracking and spalling of the concrete. As cracks grow, concrete permeability increases allowing greater access of chlorides to the steel. The cracks can also cause significant loss of bond between the reinforcing steel and the concrete.

4

Corrosion of steel in concrete is an electrochemical process that involves the transfer of ions. Electrochemical corrosion requires four factors: an anode, a cathode, an electrolyte, and an electronic circuit. The anode and cathode are different sites in the reinforcing steel. They can be located either on the same bar or on different bars. The electrolyte is usually the moisture in the concrete, and the electrical contact between different bars can be provided by steel wire ties or chair supports. To protect the steel against corrosion, at least one of these factors must be eliminated.

The type of corrosion that occurs when the anode and the cathode are located on the same bar is called *microcell* corrosion. *Macrocell* corrosion occurs when the anode and the cathode are located on different bars, such as two different layers of steel.

In reinforcing steel, when oxygen is present, iron is oxidized at the anodic site and releases electrons [Eq. (1.1)]. At the cathode, oxygen combines with moisture and the electrons released at the anode to form hydroxyl ions [Eq. (1.2)].

$$Fe \rightarrow Fe^{2+} + 2e^- \tag{1.1}$$

$$^{1}/_{2}O_2 + H_2O + 2e^- \rightarrow 2OH^- \tag{1.2}$$

The ferrous ions combine with hydroxyl ions to produce ferrous hydroxide [Eq. (1.3)]. The ferrous hydroxide is oxidized in the presence of moisture and oxygen to produce ferric hydroxide [Eq. (1.4)]. The ferric hydroxide can dehydrate to form ferric oxide, which is the red-brown oxide commonly known as rust [Eq. (1.5)].

$$Fe^{2+} + 2OH^- \rightarrow Fe(OH)_2 \tag{1.3}$$

$$4Fe(OH)_2 + 2H_2O + O_2 \rightarrow 4Fe(OH)_3 \tag{1.4}$$

$$2Fe(OH)_3 \rightarrow Fe_2O_3 + 3H_2O \tag{1.5}$$

Reinforcing steel in concrete is passive due to the high alkalinity of the cement paste in concrete (pH = 13.0 to 13.5). This high alkalinity leads to the formation of a γ-ferric oxide passive film on the surface of the steel that protects it from corrosion.

$$Fe(OH)_2 + O_2 \rightarrow \gamma\text{-}FeOOH + H_2O \qquad\qquad (1.6)$$
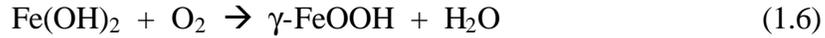
This passive film can be destroyed by two mechanisms: (1) the presence of chloride ions, which results in a localized breakdown of the passive film, and (2) carbonation, which results in a decrease in the pH of the concrete, thus reducing the passivity.

On a concrete slab, chlorides typically enter from the top surface. Once chlorides reach the top mat of steel, its electrochemical or corrosion potential with respect to a standard electrode will drop, becoming more negative. The potential of the bottom mat of steel will retain a more positive value. This difference in potential results in the formation of a galvanic cell that drives the corrosion process.

In the presence of chlorides, iron at the anode is oxidixed as before [Eq. (1.1)] and the ferrous ions react with chloride ions to form a soluble iron-chloride complex [Eq. (1.7)]. The iron-chloride complex reacts with hydroxyl ions and forms ferrous hydroxide [Eq. (1.8)], which is a greenish black product.

$$Fe^{2+} + 2Cl^- \rightarrow [FeCl\ complex]^+ \qquad\qquad (1.7)$$

$$[FeCl\ complex]^+ + 2OH^- \rightarrow Fe(OH)_2 + Cl^- \qquad\qquad (1.8)$$

The ferrous hydroxide is oxidized to ferric hydroxide that, in turn, dehydrates to form ferric oxide, as shown in Equations (1.4) and (1.5). At the cathode, hydroxyl ions are formed when oxygen combines with moisture and the electrons released at the anode as before [Eq. (1.2)]. As demonstrated by Equations (1.7) and (1.8), the chloride ions are not consumed and remain available to continue contributing to corrosion. Chloride attack on reinforcing steel

usually occurs as pitting corrosion. Pitting will continue to increase if the chloride content

exceeds a specific concentration. This chloride threshold is believed to be dependent on the

concentration of hydroxyl ions (Hausmann 1967).

1.3   Corrosion Monitoring Methods

The corrosion of metals can be evaluated using a number of methods. These include measuring

corrosion potential and macrocell corrosion rate, linear polarization resistance, electrochemical

impedance spectroscopy, and visual inspection. The following is a brief description of each

method.

1.3.1   Corrosion Potential

The electrochemical potential of a metal is a measure of its thermodynamic state and its

tendency to corrode. It is measured in volts. The more negative the potential, the higher the

tendency to corrode. The potential serves as an indicator rather than as a direct measure of the

corrosion rate. When a macrocell is formed, the driving force is the difference in potential

between the anodic and cathodic sites. As the potential difference increases with all other

variables constant, so does the corrosion rate of the bars, and the anode will always have a more

negative potential than the cathode.

The corrosion potential of a bar is obtained by measuring the potential difference

between the bar and a reference electrode. A reference electrode "has a relatively fixed value of

potential, regardless of the environment" (Uhlig 1985) and often consists of a metal that is

submerged in a solution containing its own ions. The reaction that takes place in the standard

hydrogen electrode (SHE) [Eq. (1.9)] has been chosen to represent "zero potential". The reaction

that occurs in a reference electrode is always known and so is its *half-cell potential* with respect

to the standard hydrogen electrode.

$$2H^+ + 2e^- \rightarrow H_2 \qquad\qquad (1.9)$$

Other electrodes have been developed and are used more frequently than the SHE. The two reference electrodes most commonly used are the saturated calomel electrode (SCE) and the copper-copper sulfate electrode (CSE). The differences in potential between the SHE and these two electrodes, as well as their half-cell reactions, are shown in Table 1.1.

TABLE 1.1: Standard Reference Electrodes

Electrode	Half-cell reaction	Potential vs. SHE (V)
Copper-copper sulfate (CSE)	$CuSO_4 + 2e^- \rightarrow Cu + SO_4^{2-}$	+0.318
Saturated calomel (SCE)	$HgCl_2 + 2e^- \rightarrow 2Hg + 2Cl^-$	+0.241
Standard hydrogen (SHE)	$2H^+ + 2e^- \rightarrow H_2$	0.000

The potential of a metal indicates its tendency to corrode in a given environment. ASTM C 876 is used to evaluate the corrosion potential of uncoated reinforcing steel in concrete. Table 1.2 shows the probability of corrosion based on potential measurements, as presented in ASTM C 876.

TABLE 1.2: Interpretation of Half Cell Readings (ASTM C 876)

Half-Cell Reading (V)		Interpretation
CSE	SCE	
< -0.200	< -0.125	greater than 90% probability that corrosion is not ocurring
-0.200 to -0.350	-0.125 to -0.275	corrosion activity is uncertain
> -0.350	> -0.275	greater than 90% probability that corrosion is ocurring

1.3.2 Macrocell Corrosion Rate

The corrosion rate of a reinforcing bar in a corrosion test where the corrosion current density has been measured can be obtained using Faraday's law as follows:

$$Rate = K \cdot \frac{i_c \cdot a}{n \cdot F \cdot D} \qquad\qquad (1.10)$$

8

where *Rate* is given in μm/year, and

K = conversion factor = $31.5 \cdot 10^4$ amp·μm ·sec/μA·cm·year

i_c = corrosion current density, μA/cm^2

a = atomic weight of the metal

For iron, a = 55.8 g/g-atom

n = number of ion equivalents exchanged

For iron, n = 2 equivalents

F = Faraday's constant

F = 96500 Coulombs/equivalent

D = density of the metal, g/cm^3

For iron, D = 7.87 g/cm^3

Using Eq. (1.10), the corrosion rate for iron can be expressed in terms of the corrosion current density:

$$Rate = i_c \cdot \left(\frac{1\,\text{equiv}}{96500\ \text{amp} \cdot \text{sec}} \right) \cdot \left(\frac{55.8\,\text{g}}{2\,\text{equiv}} \right) \cdot \left(\frac{\text{cm}^3}{7.87\,\text{g}} \right) \cdot \left(\frac{10^4\,\mu\text{m}}{1\,\text{cm}} \right) \cdot \left(\frac{31.5 \cdot 10^6\,\text{sec}}{\text{year}} \right) \qquad (1.11)$$

$$Rate = 11.6 \cdot i_c \qquad (1.12)$$

In a test where a macrocell is formed, the corrosion current density can be obtained by measuring the voltage drop across a resistor that connects the anode and the cathode within the cell

$$i_c = \frac{V}{R \cdot A} \qquad (1.13)$$

where

V = voltage drop across the resistor, mV

R = resistance of the resistor, ohm

A = area of exposed metal at the anode bar, cm^2

1.3.3   Polarization Resistance

The corrosion current density can also be obtained in a polarization resistance test. A potentiostat can be used to impose a range of potentials on the metal, usually –10 to +10 mV versus the open circuit corrosion potential, and measure the corresponding corrosion current. A polarization curve is obtained and a portion of this curve is linear. The slope of the linear portion of the curve is called the polarization resistance, R_p, and is proportional to the corrosion resistance of the metal. The corrosion current density is:

$$i_c = \frac{B}{R_p} \qquad\qquad (1.14)$$

where

i_c = corrosion current density, $\mu A/cm^2$,

B = constant with a value of 26 to 52 mV for steel in concrete, Tafel slope [see Jones (1996) for additional discussion].

R_p = polarization resistance (slope of linear portion of polarization curve), $k\Omega \cdot cm^2$.

The corrosion rate is then determined using Eq. (1.10). Polarization resistance can be used to determine the total corrosion rate for a metal, which will be the sum of the macrocell and microcell corrosion rates.

1.3.4   Electrochemical Impedance Spectroscopy

A potentiostat is used to apply an alternating current to the system. The different constituents of reinforced concrete (concrete, reinforcing steel, and coatings) can be modeled as a network of capacitances and resistances. When an alternating current is applied, each constituent can be evaluated independently for its contribution to the corrosion resistance of the system.

1.4 Corrosion Tests

Two rapid evaluations tests; the corrosion potential and corrosion macrocell tests; and three bench-scale tests; the Southern Exposure, cracked beam, and ASTM G 109 tests; are used to evaluate the corrosion performance of the steel. These tests use corrosion potential and corrosion rate to evaluate the performance of the steels. Full details of the specimens and testing procedures are given in Chapter 2.

1.4.1 Rapid Evaluation Tests

The rapid corrosion potential and macrocell tests were developed by Martinez et al. (1990). Their research included the development and evaluation of a standard test specimen and the use of the corrosion potential and corrosion macrocell tests to evaluate the effect of different concentrations of three deicing chemicals (calcium chloride, sodium chloride, and calcium magnesium acetate) on the corrosion of reinforcing steel cast in mortar.

The specimen used in the rapid evaluation tests consisted of a 127 mm (5 in) long, No. 13 [No. 4] reinforcing bar, partly embedded in mortar. The specimen had a thin mortar cover to allow the chlorides to reach the steel in a short period of time. The corrosion potential test determines the relative tendency of a material to corrode in a given environment. The corrosion potential was measured versus a saturated calomel electrode. The macrocell test is used to measure the corrosion rate of steel.

In the early work, the corrosion potential test provided more consistent results than the macrocell test and additional modifications to the macrocell test were recommended. Based on the test results for the different deicers, calcium chloride was observed to be more aggressive than sodium chloride, while calcium magnesium acetate was the least corrosive. The tests and test specimens have been modified in subsequent studies (Senecal et al. 1995, Schwensen et al.

11

1995, Smith et al. 1995, Kahrs et al. 2001, Darwin et al. 2002) to improve the consistency and repeatability of the results.

1.4.2   Bench-Scale Tests

Bench-scale tests include the Southern Exposure (SE), cracked beam (CB), and ASTM G 109 tests. These tests simulate the conditions found in concrete bridge decks subjected to deicing chemicals. Bench-scale specimens consist of a small concrete slab containing two mats of steel. The slabs are subjected to alternate ponding and drying cycles with a salt solution. The macrocell current between the two mats of steel is measured to obtain the corrosion rate of the bars (Section 1.3.2). The corrosion potential of the top and bottom mats is also recorded.

The Southern Exposure (SE) specimen consists of a concrete slab, 305 mm (12 in) long, 305 mm (12 in) wide, and 178 mm (7 in) high. The cracked beam (CB) specimen is the same length and height as the SE specimen, but half the width. A crack is simulated in the concrete, parallel to and above the top bar, using a 0.30 mm (0.012 in) stainless steel shim, 152 mm (6 in) long, cast into the concrete and removed 24 hours after casting. In both specimens, a concrete dam is cast around the top edge of the specimen at the same time as the specimen is cast. The ASTM G 109 specimen consists of a concrete slab, 279 mm (11 in) long, 152 mm (6 in) wide, and 114 mm (4.5 in) high. A plexiglass dam is used to pond a solution on the top of the specimen over a region with dimensions of 76 x 150 mm (3 x 6 in).

The SE tests were originally used by Pfeifer et al. (1981) in a study to evaluate concrete sealers for bridges. The test was developed to simulate the exposure conditions in southern climates, thus the name Southern Exposure. A flexural crack was induced in some specimens to evaluate the behavior of cracked concrete. The cycle for these tests consisted of ponding the specimens for 100 hours with a 15 percent NaCl solution followed by drying in a heat chamber

at 100°F for 68 hours. This weekly cycle was repeated 24 times. The ASTM G 109 test was developed to evaluate the effect of chemical admixtures on the corrosion of metals in concrete and follows a cycle that includes ponding the specimens for two weeks. After this period the specimens are allowed to dry for two weeks and the cycle is repeated until a corrosion current between the two mats of steel of 10 μA (equivalent to a current density of 0.072 μA/cm^2 and a corrosion rate of 0.83 μm/year for a No. 16 [No. 5] bar) is measured on at least half the specimens.

Tourney et al. (1993) used the G 109 test to evaluate different corrosion inhibiting admixtures. Slabs in which a flexural crack was induced on top of the steel, similar to the CB specimen, were also used in the test program. Nmai et al. (1994) used the SE test evaluate if sodium thiocyanate-based accelerating admixtures are safe for use in reinforced concrete structures. The SE and CB tests have been used at the University of Kansas in the earlier tests of microalloyed steel (Darwin 1995, Senecal et. al, 1995), as mentioned in Section 1.1, and are currently in use to evaluate several corrosion protection systems. McDonald et al. (1998) used SE and CB tests to evaluate epoxy-coated, metallic-clad, and solid metallic reinforcing bars in concrete. In that study, certain modifications in the procedures were performed, which included 12 weeks of continuous ponding after the first 12 weeks of cyclic ponding and drying, and the extension of the testing period to 96 weeks.

1.5   Objective and Scope

The corrosion resistance of three microalloyed and two conventional reinforcing steels in concrete was evaluated. The five types of reinforcing steel, provided by Gerdau AmeriSteel Corporation, include: conventional normalized steel, Thermex treated conventional steel, Thermex treated microalloyed steel with a high phosphorus content, Thermex treated

13

microalloyed steel with a high phosphorus content, and Thermex treated microalloyed steel with normal phosphorus content. A principal objective of the study was to determine if the new steels possess enough advantage over conventional steels to justify additional studies that include evaluating the new steels with epoxy coatings as suggested in prior work (Darwin 1995).

Two rapid evaluation tests, the corrosion potential and corrosion macrocell tests, and three bench-scale tests, the Southern Exposure, cracked beam, and ASTM G 109 tests, were used to evaluate the reinforcing steel.

Fifty-five corrosion potential tests were performed, five tests for each steel type in the bare condition in a 1.6 m ion NaCl and simulated concrete pore solution and three tests for each steel type with a mortar cover in 0.4 and 1.6 m ion NaCl and simulated concrete pore solutions.

One hundred fifteen macrocell tests were performed; five bare bar tests for each steel type in 1.6 m ion NaCl solution, four mortar-encased bar tests for each steel type with the ends covered with an epoxy-filled cap in 0.4 and 1.6 m ion NaCl solutions, and five mortar-encased bar tests for each type of steel without caps in 0.4 and 1.6 m ion NaCl solutions. In all cases, the NaCl solutions were combined with simulated concrete pore solution.

Six Southern Exposure, cracked beam, and G 109 tests were performed for each type of steel. The effect of combining conventional steel with corrosion-resistant steel was also evaluated using six SE specimens with N steel in the top mat and CRPT1 in the bottom mat (N/CRPT1), and six SE specimens with CRPT1 steel in the top mat and N steel in the bottom mat (CRPT1/N).

Mechanical tests were performed to obtain the yield and tensile strength, as well as the elongation of each microalloyed steel. Bend tests were also performed.

14

Chapter 2

Experimental Work

2.1   General

The corrosion potential, corrosion macrocell, Southern Exposure, cracked beam and ASTM G

109 tests are used to compare the different types of reinforcing steel. The first two are rapid

evaluation tests, while the other three are longer-term bench-scale tests. This chapter describes

the equipment, materials, and procedures used to prepare the specimens and to monitor and

record corrosion behavior.

2.2   Reinforcing Steel

Three microalloyed steels and two conventional steels provided by Gerdau AmeriSteel are

evaluated on this study. The chemical composition and mechanical properties of the steel, as

reported by Gerdau AmeriSteel, are given in Tables 2.1 and 2.2. The types of steel are identified

as follows:

 N: conventional steel, normalized.

 T: conventional steel, Thermex treated.

 CRPT1: microalloyed steel with a high phosphorus content (0.117%), Thermex treated

   (quenched and tempered).

 CRPT2: microalloyed steel with a high phosphorus content (0.100%), Thermex treated.

 CRT: microalloyed steel with normal phosphorus content, Thermex treated.

TABLE 2.1: Chemical Composition of Reinforcing Steel, %

Designation	C	Mn	P	S	Si	Cr	Cu	Ni	Sn	Mo	V
N	0.400	1.010	0.022	0.032	0.220	0.200	0.300	0.200	0.010	0.040	0.003
T	0.360	0.770	0.018	0.040	0.160	0.180	0.310	0.140	0.004	0.042	0.004
CRPT1	0.180	0.960	0.117	0.025	0.290	0.550	0.520	0.120	0.009	0.036	0.019
CRPT2	0.160	1.010	0.100	0.033	0.290	0.650	0.560	0.140	0.010	0.035	0.013
CRT	0.190	0.940	0.017	0.031	0.390	0.710	0.450	0.110	0.009	0.040	0.002

TABLE 2.2: Mechanical Properties of Reinforcing Steel

Steel designation	Yield strength (MPa)	(ksi)	Tensile strength (MPa)	(ksi)	Elongation	Bending	Deformation height (mm)	(in.)	Weight (kg/m)	(lb/ft)
N	466.5	67.7	774.0	112.3	13.0%	OK	0.965	0.038	1.666	1.058
T	562.7	81.6	709.5	102.9	13.0%	OK	1.067	0.042	1.570	0.997
CRPT1	616.1	89.4	769.5	111.6	13.0%	OK	0.940/0.1.041 [a]	0.037/0.041 [a]	1.568/1.587 [a]	0.996/1.008 [a]
CRPT2	607.2	88.1	756.4	109.7	12.5%	OK	0.991/0.1.067 [a]	0.039/0.042 [a]	1.559/1.678 [a]	0.990/1.066 [a]
CRT	600.2	87.1	765.1	111.0	12.0%	OK	0.1.016/1.067 [a]	0.040/0.042 [a]	1.562/1.587 [a]	0.992/1.008 [a]

[a] Information for two different rollings

2.3   Rapid Evaluation Tests

The rapid evaluation tests used in this study are the corrosion potential and the corrosion macrocell tests. Bars were tested with and without a mortar cover at two different NaCl ion concentrations (0.4 m and 1.6 m). The study included 55 corrosion potential tests and 115 macrocell tests. This section includes a description of the test procedures, the test specimens, and the equipment and materials required for the tests.

2.3.1   Test Procedures

2.3.1.1 Corrosion Potential Test

The corrosion potential test determines the relative tendency of a material to corrode in a given environment. The corrosion potential of the reinforcing bars in 0.4 and 1.6 m

ion NaCl solutions is measured with respect to a saturated calomel electrode in a saturated potassium chloride solution. Readings are taken daily.

As shown in Figure 2.1, the specimen is placed in the center of a container and fixed in place with the help of a styrofoam support. In the case of the mortar specimens (shown in Figure 2.1), the specimen is surrounded with mortar fill. Mortar fill is not used for bare bar specimens. The simulated concrete pore solution with NaCl is added to the container until the level of the solution is 51 mm (2 in.) from the top of the bar for bare specimens and 13 mm ($^1/_2$ in.) from the top of the steel-mortar interface for mortar-encased specimens. The free end of a copper wire attached to the specimen is threaded through the container lid and then attached to a binding post on the terminal box. A salt bridge connects the solution surrounding the specimen with the solution surrounding the electrode, which is placed in another container with saturated potassium chloride solution.

Voltage readings are taken by connecting the saturated calomel electrode to the positive terminal on the voltmeter and the negative terminal of the voltmeter to the specimen through a binding post in a terminal box.
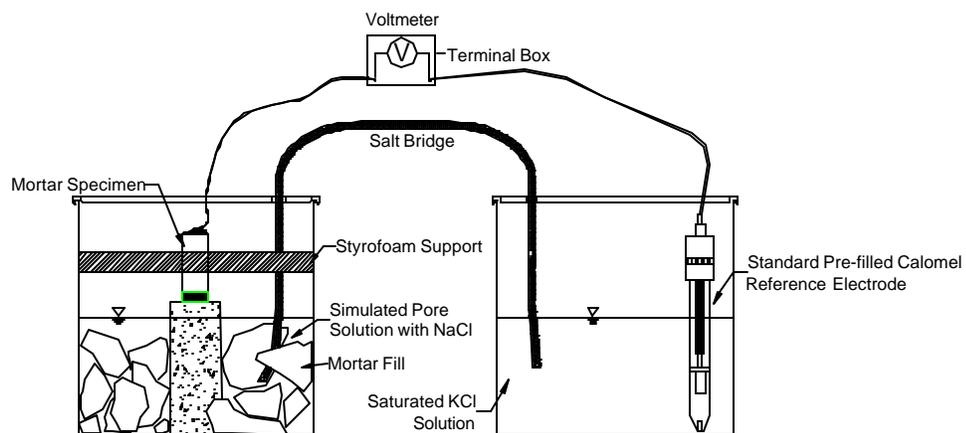
FIGURE 2.1: Corrosion Potential Test Setup with Mortar Specimen

2.3.1.2 Corrosion Macrocell Test

The corrosion macrocell test is used to measure the corrosion rate of steel. As shown in Figures 2.2 and 2.3, the macrocell consists of an anode and a cathode. The cathode is made up of two specimens in simulated concrete pore solution. The anode consists of one specimen in simulated concrete pore solution with sodium chloride (0.4 or 1.6 m ion concentration). Corrosion potentials of the anode and cathode with respect to a saturated calomel reference electrode (SCE) are also recorded. The tests run for 100 days. Tests are performed on bare bars, mortar-encased specimens with epoxy-filled caps on the ends of the bars, and mortar specimens without caps on the ends.

For the anode, one specimen is placed in the center of a container. In the case of mortar-encased specimens, the specimen is surrounded with mortar fill. The top of the bar is supported with styrofoam. As in the corrosion potential test, the simulated concrete pore solution with NaCl is added to the container until the level of the solution is 51 mm (2 in.) from the top of the bar for bare specimens, and 13 mm ($^1/_2$ in.) from the top of the steel-mortar interface for mortar specimens. The free end of a copper wire attached to the specimen is threaded through the container lid and then attached to a black binding post in a terminal box. Two specimens are placed in another container to act as the cathode. Mortar specimens are surrounded with mortar fill. The bars are fixed in place with the help of a styrofoam support. Simulated concrete pore solution is added to the container until the level of the solution is the same as in the other container. The free ends of copper wires attached to the specimens are threaded through the container lid and then attached to a third wire that has its other end attached to a red binding post in a terminal box. Air, scrubbed to remove CO_2, is bubbled into the solution surrounding the

cathode specimens to provide enough oxygen for the cathodic reaction. A salt bridge connects

the solution surrounding the cathode and the anode.
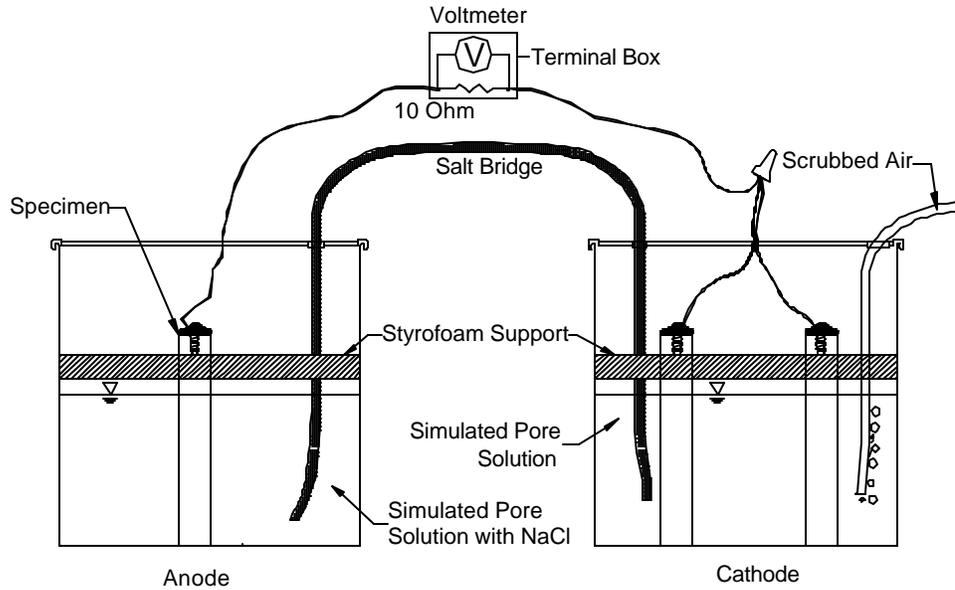
FIGURE 2.2: Macrocell Test Setup with Bare Bars
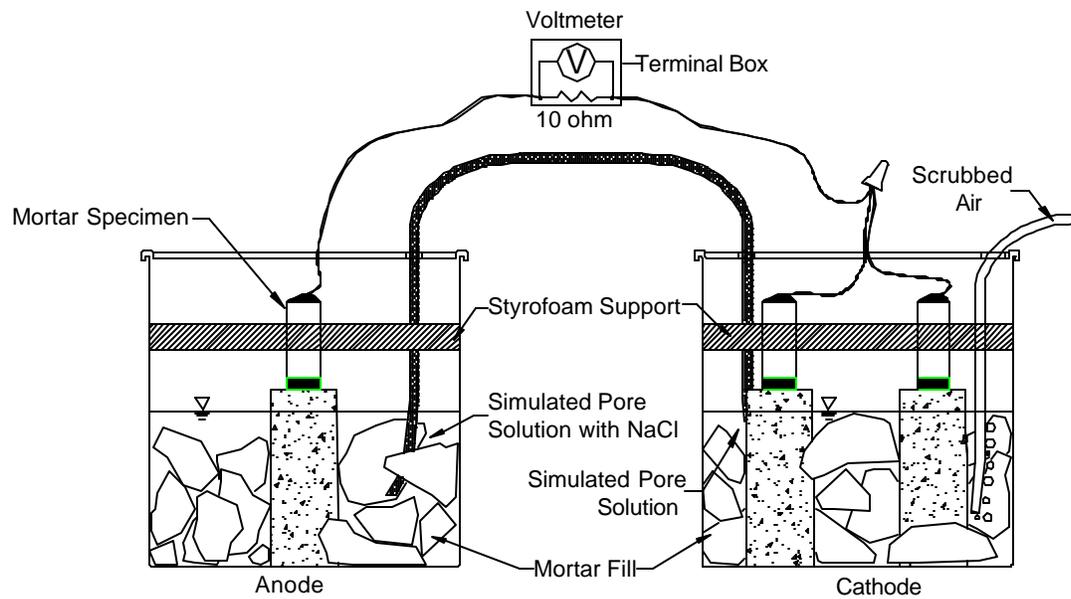
FIGURE 2.3: Macrocell Test Setup with Mortar Specimens

The voltage drop is measured across a 10-ohm resistor that completes the macrocell circuit by connecting the black binding post to the red binding post in the terminal box. The negative terminal of the voltmeter is connected to the black binding post and the positive terminal of the voltmeter is connected to the red binding post. After the voltage drop reading has been measured, the anodes are disconnected from the terminal box. Two hours after being disconnected, corrosion potentials of the anode and the cathode are measured by placing the saturated calomel electrode in the solution surrounding the bar and connecting it to the positive terminal on the voltmeter and the bar (cathode or anode) to the negative terminal of the voltmeter. Figure 2.4 shows the setup of the macrocell test when measuring the corrosion potential of the anode.
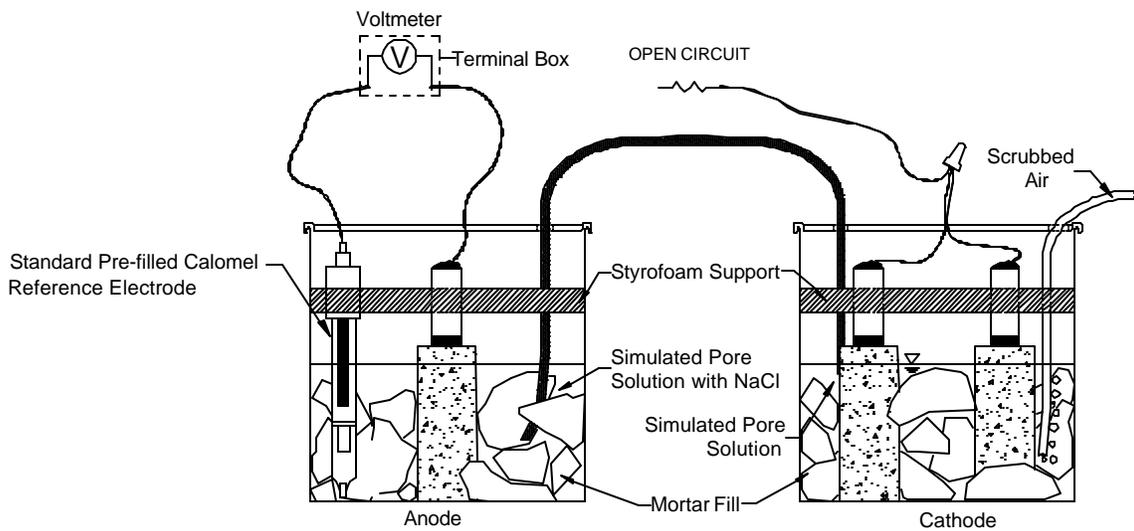
FIGURE 2.4: Macrocell Test Setup for Corrosion Potential Readings

As described in Chapter 1, the voltage drop obtained from the macrocell readings is converted to a corrosion rate (in μm/year) using the following formula:

$$Rate = 11.6 \cdot i_c = \frac{11600 \cdot V}{A \cdot R} \qquad (2.1)$$

where

i_c = corrosion current density, $\mu A/cm^2$

V = voltage drop across the resistor, mV

R = resistance of the resistor, ohm

A = area of exposed metal at the anode bar, cm^2

2.3.2   Test Specimen Preparation

The specimen used in the corrosion potential and macrocell tests consists of a 127 mm (5 in.) long, No. 16 [No. 5] reinforcing bar, either bare or partly embedded in mortar, as shown in Figure 2.5. Sharp edges on the bar ends are removed with a grinder, and the bar is drilled and tapped at one end to receive a 10-24 threaded bolt, 10 mm ($^3/_8$ in.) long, which is used to connect the copper wire.
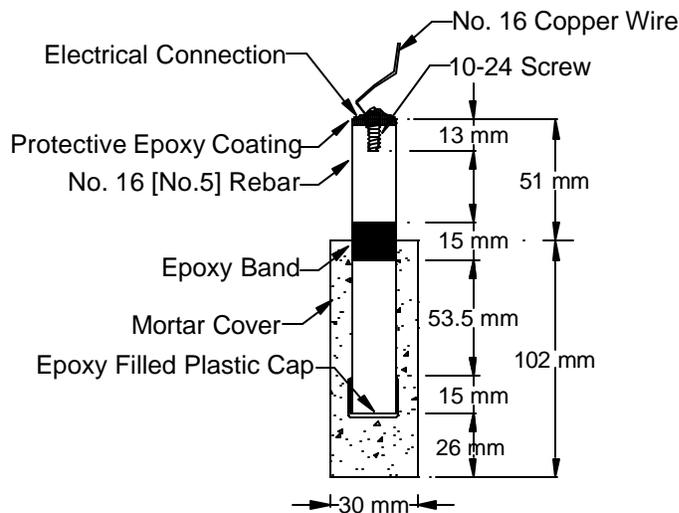
FIGURE 2.5: Mortar Specimen

21

The bar is then cleaned with acetone to remove oil or dust from the bar surface. Sections of the bar that will be covered with epoxy are sandblasted to provide a better surface for the epoxy to adhere. These sections include the tapped end of the bar, and for mortar-encased bars, a 15 mm (0.60 in.) wide band centered 51 mm (2 in.) from the tapped end of the bar, and in some cases, the unthreaded end of the bar. Before sandblasting, sections of the bars that will not be sandblasted are covered with duct tape to protect them. After sandblasting, the duct tape is removed and the bars are again cleaned with acetone to remove the sand. The epoxy is applied in two coats. The second coat is applied when the first coat feels tacky after approximately two hours. Some specimens had plastic caps placed on the ends. In this case, a first coat of epoxy is applied to the unthreaded end of the bar. Two hours later, a cap is half-filled with epoxy, and the end of the bar is inserted into the cap. The epoxy and caps are applied at least 24 hours before casting the bar in mortar. Since the mill scale on the bars is believed to provide some corrosion protection, caps were used to protect the ends of some specimens to prevent the areas without mill scale from exposure to the deicing chemicals. Figure 2.5 shows a sketch of the macrocell specimen with a cap on the end of the bar.

2.3.2.1 Mold Design and Assembly

The mold design was developed by Martinez et al. (1990). The mold, shown in Figure 2.6, consists of the following commercially available materials:

1)   One laboratory grade No. 6 ½ rubber stopper with a centered 16 mm ($^5/_8$ in.) diameter hole (D)

2)   One laboratory grade No. 9 rubber stopper with a centered 16 mm ($^5/_8$ in.) diameter hole (C).

3)   One ASTM D 2466 25.4 mm (1 in.) to 25.4 mm (1 in.) PVC fitting, 33 mm (1.3 in.) internal diameter. The fitting is turned in a lathe to 40.6 mm (1.6 in.) external diameter so that it will fit in an ASTM D 2466 32 mm

(1¼ in.) to 32 mm (1¼ in.), 42 mm (1.65 in.) internal diameter PVC fitting (E).

4) One ASTM D 2466 32 mm (1¼ in.) to 32 mm (1¼ in.) PVC fitting, 42 mm (1.65 in.) internal diameter, shortened by 14 mm (0.55 in.) on one end (B).

5) One ASTM D 2241 SDR 21 25.4 mm (1 in.) PVC pipe, 30 mm (1.18 in.) internal diameter, 102 mm (4 in.) long. The pipe is sliced longitudinally to allow for specimen removal. The cut in the pipe is covered with a single layer of masking tape to avoid leakage during casting (G).

6) Two pieces of 2 x 8 pressure treated lumber. Holes and recesses are bored into the flat surfaces to accept the specimen mold assembly and facilitate mortar placement (A).

7) Four threaded rods (H).

The laboratory grade rubber stoppers are used to hold the reinforcing bars in place and maintain uniform cover.
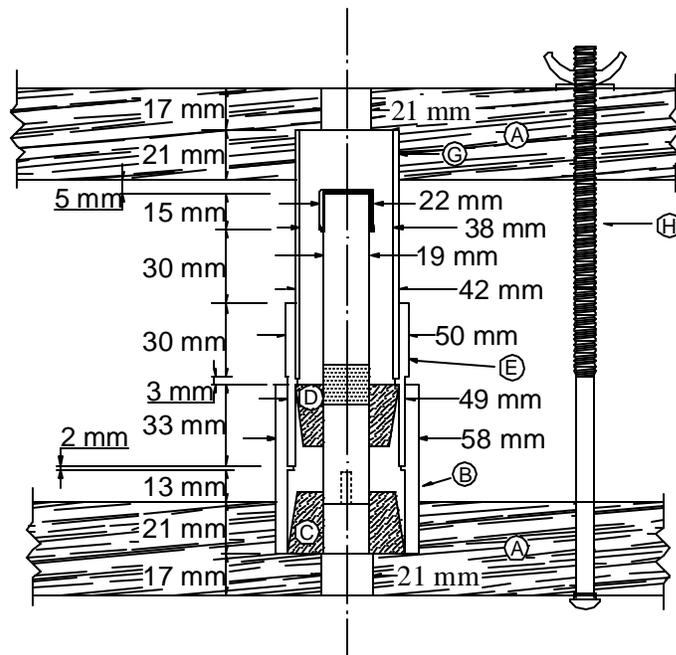
FIGURE 2.6: Mold Assembly for Mortar Speciments

The mold (Figure 2.6) is assembled as follows:

1) The tapped end of the reinforcing bar is inserted through the hole of the small rubber stopper, D, beginning at the widest end of the stopper. The distance between the untapped end of the bar and the rubber stopper is 76 mm (3 in.)

2) The rubber stopper is inserted in the machined end of the small connector, E. The widest end of the small rubber stopper has to be in contact with the shoulder (an integral ring) on the internal surface of the small connector.

3) The large rubber stopper, C, is inserted in the cut end of the larger connector, B, until it makes contact with the shoulder on the inside surface of the connector.

4) The machined end of the small connector, E, is inserted in the free end of the large connector, B. At the same time, the tapped end of the reinforcing bar is inserted through the hole of the large rubber stopper, C.

5) The longitudinal slice along the side of the PVC pipe, G, is taped with masking tape. The pipe is then inserted in the free end of the small connector.

6) The assembled mold is inserted into the recesses in the top and bottom wooden pieces of the fixture, A. The threaded rods, H, are then inserted between the wooden boards. The rods are used to hold the molds together and center the reinforcing bar by tightening or loosening the nuts on the rods.

The specimens are cast in three layers. Each layer is rodded 25 times with a 2-mm (0.080-in.) diameter rod. The rod is allowed to penetrate the previous layer of mortar. After rodding, each layer is vibrated for 30 seconds on a vibrating table with amplitude of 0.15 mm (0.006 in.) and a frequency of 60 Hz. To eliminate the effect of variations in the mortar mix, specimens for the different types of steel are cast from the same batch of mortar.

The specimens are removed from the molds 24 hours after casting and placed in lime-

saturated water for 13 days. After this period, the specimens are removed from the lime-saturated water. The tapped end of the specimen is dried with compressed air and a 16-gage copper wire is attached to the specimen with a 10-24 x 9.5 mm threaded bolt. The electrical connection is epoxy coated to prevent crevice corrosion. Two coats of epoxy are applied as described above. The epoxy is allowed to dry for one day before the tests are started.

2.3.3   Materials and Equipment

The following equipment and materials are used in the rapid evaluation tests.

- *Voltmeter:* Hewlett Packard digital voltmeter, Model 3455A, with an impedance of 2MΩ.

- *Mixer:* Hobart mixer, Model N-50. This mixer complies with ASTM C 305 and is used for mixing the mortar for the specimens used in the rapid evaluation tests.

- *Saturated Calomel Electrode (SCE):* Fisher Scientific Catalog No. 13-620-52. The reference electrode is used to measure the corrosion potential of the bars.

- *Terminal Box:* Terminal boxes are used to make the electrical connections between the test specimens. Each terminal box consists of a project box (from Radio Shack) with 5 pairs of binding posts (one red and one black). A 10-ohm resistor connects each pair of binding posts in the terminal boxes used for the macrocell tests.

- *Wire:* 16-gage insulated copper wire is used to make the electrical connections to the bars.

- *Mortar:* The mortar is made with Portland Cement Type I (ASTM C 150), ASTM C 778 graded Ottawa sand, and deionized water. The mortar has a water-cement ratio of 0.5 and a sand-cement ratio of 2. The mortar is mixed in accordance with the requirements of ASTM C 305.

    a.   **Mortar Fill***:* Mortar fill is used to surround the specimens with mortar cover. It is prepared with the same materials and mixing

procedure as the mortar for the specimens. It is cast 25 mm (1 in.) deep on a metal baking sheet. The mortar fill in the container is crushed into 25 to 50 mm (1 to 2 in.) pieces prior to use.

b. **Epoxy Coating**: A two-part epoxy coating (Nap Gard Rebar Patch Kit, manufactured by Herberts-O'Brien) is used to cover the electrical connections. It is applied in accordance with manufacturer's recommendations.

c. **Caps**: Plastic caps 16 mm ($^5/_8$ in.) in diameter and 15 mm (0.6 in.) long (from ACE hardware) are used to cover the ends of the bars in some mortar specimens.

d. **Concrete Pore Solution**: The simulated concrete pore solution is prepared based on the analysis by Farzammehr (1985) which states that one liter of pore solution contains 974.8 g of distilled water, 18.81 g of potassium hydroxide (KOH), 17.87 g of sodium hydroxide (NaOH), and 0.14 g of sodium chloride (NaCl). The amounts used in the present study differ from those measured by Farzammehr, providing a somewhat lower pH solution. One liter of pore solution contains 974.8 g of distilled water, 16.34 g of potassium hydroxide (KOH), and 17.54 g of sodium hydroxide (NaCl). Following the procedures used by Senecal et al. (1995) and Schwensen et al. (1995), NaCl is not used in the simulated pore solution.

e. **Sodium Chloride Solution**: The sodium chloride solutions are used in both the corrosion potential and macrocell tests. They are prepared by adding 11.4 or 45.6 g of NaCl to one liter of simulated concrete pore solution to obtain 0.4 and 1.6 molal ion concentration solutions, respectively.

f. **Salt Bridges**: Salt bridges are used to provide an ionic path between the solutions surrounding the cathode and the anode in the macrocell tests, and between the solution surrounding the specimen and the solution surrounding the reference electrode in

the corrosion potential tests. They are prepared following a procedure described by Steinbach and King (1950). A salt bridge consists of a flexible latex tube with an inner diameter of 9.5 mm ($^3/_8$ in.), filled with a gel. The gel is made using 4.5 g of agar, 30 g of potassium chloride (KCl), and 100 g of distilled water, enough to produce 4 salt bridges, each with a length of 0.6 m (2 ft). Salt bridges are prepared by mixing the constituents and heating them over a burner or hotplate for about 1 minute, or until the solution starts to thicken. The gel is poured into the latex tubes using a funnel. The salt bridges are then placed in boiling water for one hour, keeping the ends of the tubes out of the water. After boiling, the salt bridges are allowed to cool until firm. To provide an adequate ionic path, the gel in the salt bridge must be continuous, without any air bubbles.

g. **Air Scrubber**: Air is bubbled into the simulated concrete pore solution surrounding the cathode in the macrocells to provide enough oxygen for the cathodic reaction. An air scrubber is used to prevent carbonation of the pore solution by eliminating the carbon dioxide from the air. To prepare the air scrubber, a 5 gallon container is filled with a 1M sodium hydroxide solution. Compressed air is channeled into the scrubber and out to the specimens through latex tubing. The procedure for preparing the air scrubber is as follows:

1) Two barbed fittings are inserted on the top of the container.

2) A 1.5 m (5 ft) piece of plastic tubing is cut. On one end of the tubing, 1.2 m (4 ft) is perforated with a knife, making hundreds of holes to allow the air to produce small bubbles. The end of the tubing closest to the holes is sealed with a clamp.

3) The end with the holes is coiled at the bottom of the container and trap rock is used to hold down the tubing.

The other end of the tubing is connected to the inside part of one of the barbed fittings.

4) The other side of the barbed fitting is connected to a plastic tube, which is connected to the compressed air outlet.

5) Another piece of plastic tubing is connected to the outside of the other barbed fitting. The air is distributed to the solution surrounding the cathodes using 0.3 m (1 ft) lengths of latex tubing and polypropylene T-shaped connectors.

6) Screw clamps are placed to regulate the amount of air bubbled into each container.

Distilled water is periodically added to the container to replace water that is lost due to evaporation. The pH of the solution is checked every 2 months. Additional NaOH is added as needed.

2.3.4   Test Program

A total of 55 corrosion potential tests were performed. These include five tests for each type of steel in the bare condition in 1.6 m ion NaCl solution and three for each steel with a mortar cover in each of the NaCl concentrations (0.4 and 1.6 m).

A total of 115 macrocell tests were performed. These include five bare bar tests for each type of steel in the 1.6 m ion NaCl concentration, four mortar-encased bar tests for each type of steel with the ends covered with an epoxy-filled cap in 0.4 and 1.6 m ion NaCl solutions, and five mortar-encased bar tests for each type of steel without caps, at the same concentrations.

A summary of the test program for the rapid evaluation tests is given in Tables 2.3 and 2.4.

TABLE 2.3: Corrosion Potential Test Program

Steel designation	No. of tests	NaCl concentration
Bare specimens		
N	5	1.6 m
T	5	1.6 m
CRPT1	5	1.6 m
CRPT2	5	1.6 m
CRT	5	1.6 m
Mortar specimens		
N	3	0.4 m
T	3	0.4 m
CRPT1	3	0.4 m
CRPT2	3	0.4 m
CRT	3	0.4 m
N	3	1.6 m
T	3	1.6 m
CRPT1	3	1.6 m
CRPT2	3	1.6 m
CRT	3	1.6 m

TABLE 2.4: Corrosion Macrocell Test Program

Steel designation	No. of tests	NaCl concentration
Bare specimens		
N	5	1.6 m
T	5	1.6 m
CRPT1	5	1.6 m
CRPT2	5	1.6 m
CRT	5	1.6 m
Mortar specimens with epoxy-filled caps		
N	4	0.4 m
T	4	0.4 m
CRPT1	4	0.4 m
CRPT2	4	0.4 m
CRT	4	0.4 m
N	4	1.6 m
T	4	1.6 m
CRPT1	4	1.6 m
CRPT2	4	1.6 m
CRT	4	1.6 m
Mortar specimens without caps		
N	5	0.4 m
T	5	0.4 m
CRPT1	5	0.4 m
CRPT2	5	0.4 m
CRT	5	0.4 m
N	5	1.6 m
T	5	1.6 m
CRPT1	5	1.6 m
CRPT2	5	1.6 m
CRT	5	1.6 m

2.4   Bench-Scale Tests

Three bench-scale tests, the Southern Exposure, cracked beam, and ASTM G 109 tests, are used

for this study. In each case, the testing period is 96 weeks. As in the rapid evaluation tests, the

specimens are monitored by measuring the corrosion rate and corrosion potential of the bars. In

addition, the mat-to-mat resistance is also recorded. A total of 102 bench-scale tests were performed.

2.4.1   Test Procedures

2.4.1.1 Southern Exposure (SE)

The Southern Exposure specimen (Figure 2.7) consists of a concrete slab, 305 mm (12 in.) long, 305 mm (12 in.) wide, and 178 mm (7 in.) high. The slab contains two mats of steel electrically connected across a 10-ohm resistor. The top mat of steel has two bars, and the bottom mat of steel has four bars. A concrete dam is cast around the top edge of the specimen at the same time as the specimen is cast. The top and bottom concrete cover is 25.4 mm (1 in.).
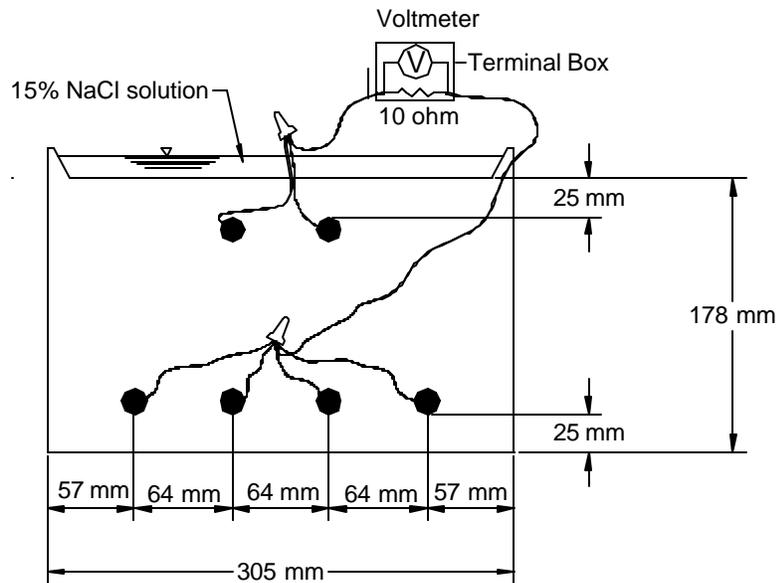
FIGURE 2.7: Southern Exposure Specimen

2.4.1.2 Cracked Beam (CB)

The cracked beam specimen (Figure 2.8a) is the same length and height as the SE specimen, but half the width. It contains one bar in the top mat electrically connected across a 10-ohm resistor to two bars in the bottom mat. A crack is simulated in the concrete parallel to and above the top bar using a 0.30 mm (0.012 in.) stainless steel shim, 152 mm (6 in.) long, cast

into the concrete and removed 24 hours after casting. As in the Southern Exposure specimen, the concrete cover to the top and bottom steel is 25.4 mm (1 in.).

2.4.1.3 ASTM G 109

ASTM G 109 was developed to test the effect of chemical admixtures on the corrosion of metals in concrete. The specimen (Figure 2.8b) has the following dimensions: 279 mm (11 in.) x 153 mm (6 in.) x 114 mm (4.5 in.). The specimen contains two layers of bars; the top layer has one bar with a 25.4 mm (1 in.) top concrete cover and the bottom layer contains 2 bars with a bottom concrete cover of 25.4 mm (1 in.). The two layers are electrically connected across a 100-ohm resistor. A plexiglass dam is used to pond a solution on the top of the specimen over a region with dimensions of 76 x 150 mm (3 x 6 in.).
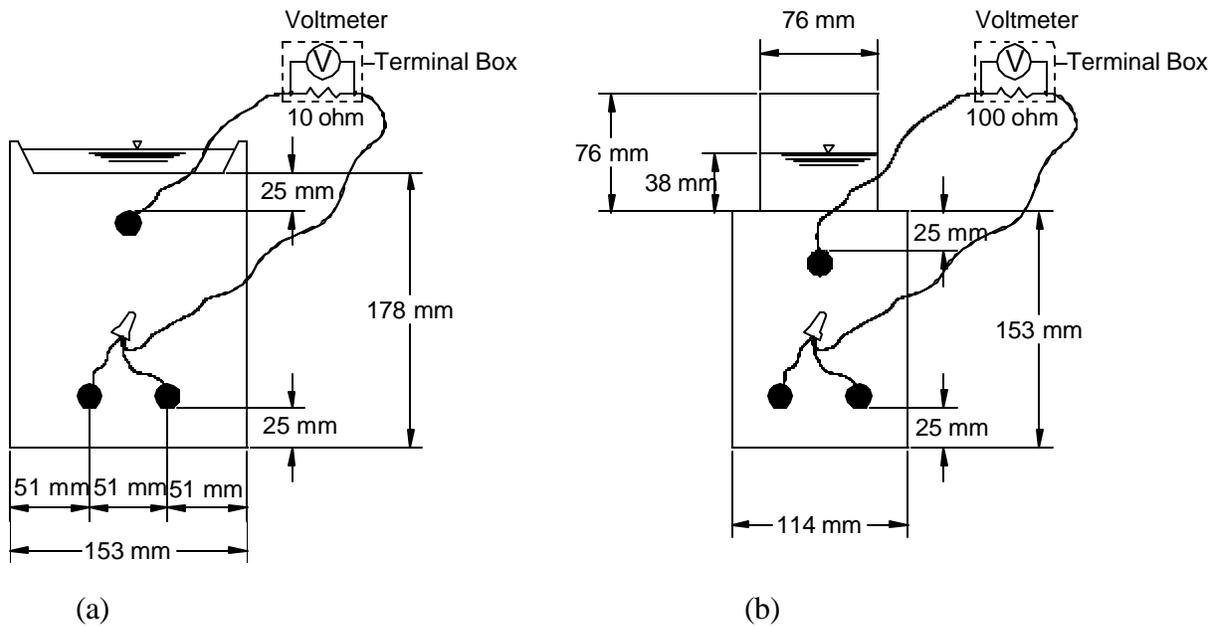
FIGURE 2.8(a): Cracked Beam Specimen

FIGURE 2.8(b): G 109 Specimen

2.4.1.4 Procedure for Southern Exposure (SE) and Cracked Beam (CB) Tests

The test procedure for the Southern Exposure and cracked beam specimens proceeds as follows:

1) On the first day, the specimens are ponded with a 15% NaCl solution at room temperature, 20 to 29°C (68 to 84°F).   This solution is left on the specimen for 4 days.

2) On the fourth day, the voltage drop across the 10-ohm resistor connecting the two mats of steel is recorded for each specimen. The circuit is then disconnected and the mat-to-mat resistance is recorded. Two hours after disconnecting the specimens, the solution on top of the specimens is removed and the corrosion potentials with respect to a copper-copper sulfate electrode (CSE) of the top and bottom mats of steel are recorded.

3) After the readings have been obtained, a heat tent is placed over the specimens, which maintains a temperature of 38 $\pm$ 2°C (100 $\pm$ 3°F) The specimens remain under the heat tent for three days.

4) After three days, the tent is removed and the specimens are again ponded with a 15% NaCl solution, and the cycle starts again.

5) This cycle is repeated for 12 weeks. The specimens are then subjected to 12 weeks of continuous ponding. During this period the solution is not removed and the specimens are not placed under the heat tents. The corrosion potential during this period is taken with respect to a saturated calomel reference electrode (SCE) instead of a copper-copper sulfate electrode (CSE), because the SCE is more convenient when the electrode has to be immersed in solution.

After 12 weeks of continuous ponding, the drying and ponding cycle is repeated for 12 weeks, followed by 12 weeks of continuous ponding. This 24 week cycle is repeated to complete 96 weeks of testing.

2.1.4.5 Test Procedure for ASTM G 109 Test

The ponding and drying cycles in the G 109 test differ from those used in the Southern Exposure (SE) and cracked beam (CB) tests. For the G 109 test, the specimens are ponded with a 3% NaCl solution for two weeks. After two weeks the solution is removed and the specimens are allowed to dry for two weeks. This cycle is repeated for the full test period. The same readings as obtained for the Southern Exposure and cracked beam tests are taken weekly.

2.4.2   Test Specimen Preparation

The procedure for preparing the bench-scale specimens is as follows.

1)   The bars are cut to the desired length, 305 mm (12 in.) for Southern Exposure and cracked beam specimens and 279 mm (11 in.) for G 109 specimens.

2)   The sharp edges on the ends of the bars are removed with a grinder.

3)   The ends of the bars are drilled and tapped to receive a 10-24 threaded bolt, 10 mm ($^3/_8$ in.) long. The bolt is used to hold the bars in place during casting and to make an electrical connection during the testing period.

4)   The bars are then cleaned with acetone to remove dust and oil. The bars used in the G 109 test are pickled in a 10% sulfuric acid solution for 10 minutes and then dried and wire brushed. The procedure in the present study deviates from ASTM G 109 in two ways. First, the bars do not project out of the specimen. Second, electroplater's tape is not used to cover part of the bars, as described in the standard.

5)   Mineral oil is applied to the wooden forms prior to placing the bars in the forms.

6)   For the cracked beam specimens, a 0.30 mm stainless steel shim is fixed on to the bottom part of the form so that the shim is located underneath and parallel to the top bar.

7)   The bars are bolted into the forms. The Southern Exposure and cracked

beam specimens are cast upside down to allow for the integral concrete dam to be cast at the same time. The ASTM G 109 specimens are also cast upside down to provide a smooth surface for attaching the plexiglass dams.

The specimens are cast using the following procedure:

1) The concrete is mixed following the procedure in described in ASTM C 192.

2) The specimens are cast in two layers. Each layer is vibrated for 30 seconds on a vibrating table with an amplitude of 0.15 mm (0.006 in) and a frequency of 60 Hz. Specimens for the different types of steel are cast using the same concrete batch to eliminate the effect of variations in the concrete mix on the test results.

3) After the second layer is vibrated, the surface of the specimen is finished using a wooden float.

4) The specimens are cured in air for 24 hours.

5) After 24 hours, the Southern Exposure and cracked beam specimens are removed from the molds and the stainless steel shims are removed from the cracked beam specimens. The specimens are placed in a plastic bag with distilled water for 48 hours and then removed from the bags and cured in air for 25 days. After the first 24 hours, the G 109 specimens are removed from the molds and placed in a curing room, with a temperature of $23 \pm 2^{o}C$ ($73.4 \pm 3.6^{o}F$) and a relative humidity above 95%, for 26 days.

6) Several days before the testing period starts, 16-gage insulated copper wire is attached to the bars in the specimens using 10-24 threaded bolts, 10 mm ($^{3}/_{8}$ in.) long. The sides of the specimens are then covered with epoxy, with emphasis on coating the electrical connections to prevent crevice corrosion or galvanic corrosion from occurring. The electrical connections are made to the bars in the G 109 specimens after the specimens have been removed from the curing room.

7)   The top of the specimens is lightly sanded.

8)   The specimens are supported on two pieces of wood, at least 13 mm (2 in.) thick, to allow air to flow under the specimens.

9)   Plexiglass dams are attached to top of the G 109 specimens using superglue. The joints are sealed with silicone.

10)   The top layer of steel is then connected to the outside red binding post on the terminal box, while the bottom layer of steel is connected to the outside black binding post (Figure 2.9)

2.4.3   Equipment and Materials

The following equipment and materials are used in the bench-scale tests.

- **Voltmeter**: Hewlett Packard digital voltmeter, Model 3455A, with an impedance of 2MΩ.

- **Ohmmeter**: Hewlett Packard digital milliohmmeter, Model 4338A.

- **Mixer**: Lancaster, counter current batch mixer, with a capacity of 0.06 m^3 (2 ft^3).

- **Saturatel Calomel Electrode (SCE)**: Fisher Scientific Catalog No. 13-620-52. The saturated calomel electode was used to take potential readings during the continuous ponding cycle.

- **Copper-Copper Sulfate Electrode (CSE)**: MC Miller Co. Electrode Model RE-5. The copper-copper sulfate electrode was used to take potential readings during the ponding and drying cycle.

- **Epoxy**: Ceilgard 615 provided by Ceilcote. The epoxy is used to cover the sides of the specimens and the electrical connections to the specimen.

- **Concrete**: The concrete consists of Portland Type I cement, crushed limestone obtained from Fogle Quarry [¾ in. nominal maximum size, SG(SSD) = 2.58, absorption = 2.27%, unit weight = 1536 kg/m^3 (95.9 lb/ft^3)] as coarse aggregate, Kansas river sand (fineness modulus = 2.51, SG(SSD) = 2.60, absorption = 0.78%) as fine aggregate, tap water, and

vinsol rensin as air-entraining agent. The concrete has a water-cement ratio of 0.45, and the following proportions:

- Water: 160 kg/m^3 (269 lb/yd^3)
- Cement: 355 kg/ m^3 (599 lb/yd^3)
- Fine aggregate: 852 kg/ m^3 (1436 lb/yd^3)
- Coarse aggregate: 874 kg/ m^3 (1473 lb/yd^3)
- Vinsol rensin: 90 mL/m^3 (70 mL/yd^3)

The concrete has a slump of 3 in., an air content of 6.0%, and a unit weight of 2241 kg/m^3 (139.9 lb/ft^3).

- **Plexiglass**: Plexiglass with a wall thickness of 3 mm (0.125 in.) is used to build the plastic dams on top of the G 109 specimens.
- **Sulfuric Acid**: A 10% solution by weight of sulfuric acid is used to pickle the bars for the G 109 test.
- **Terminal Box**: As in the macrocell tests, a terminal box was prepared and used to make electrical connections between specimens. In this case, it was made up of a project box obtained from Radio Shack with 6 sets of 3 binding posts attached to it. Binding posts were either red or black. A sketch of the setup is shown in Figure 2.9. A 10-ohm resistor for the Southern Exposure and cracked beam tests and a 100-ohm resistor for the G 109 test is placed between the outside red binding post and the inner binding post. The top layer of steel is connected to the outside red binding post, while the bottom layer of steel is connected to the outside black binding post. A 16-gage insulated copper wire connects the outside black binding post to the inside binding post. This wire is disconnected from the inside binding post when an open circuit is required for taking the corrosion potential of the bars.

BINDING POSTS

Red   Red or   Black
Black

To top mat

To bottom mat

16-gage copper
wire

16-gage copper
wire (open circuit)

16-gage copper wire
(closed circuit)
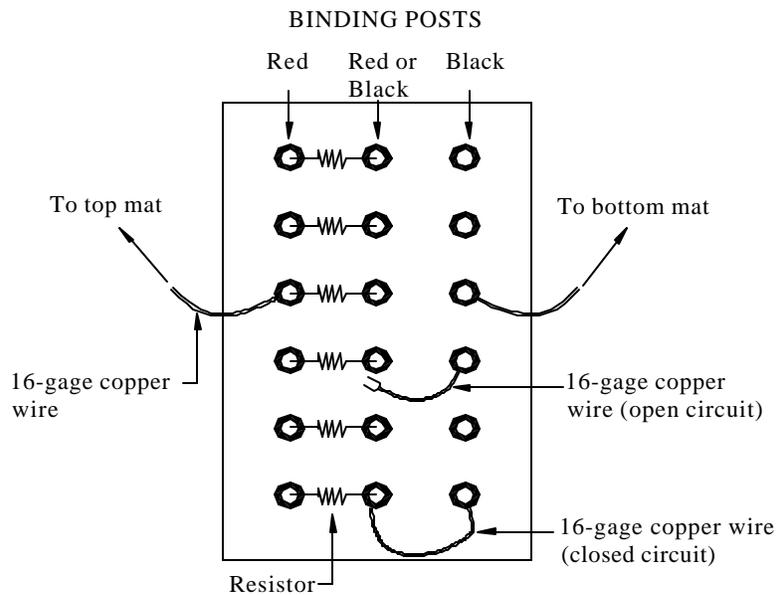
Resistor

FIGURE 2.9: Terminal Box Setup for Bench-Scale Tests

2.4.4   Test Program

Six Southern Exposure (SE), cracked beam (CB) and G 109 tests were used for each type

of steel. The effect of combining conventional steel with corrosion-resistant steel was also tested

using six SE specimens with N steel on the top mat and CRPT1 on the bottom mat (N/CRPT1)

and six SE specimens with CRPT1 steel on the top mat and N steel on the bottom mat

(CRPT1/N). The test program for the bench-scale tests is summarized in Table 2.5.

38

TABLE 2.5: Bench-Scale Test Program

Test	Steel designation	No. of tests
SE	N	6
SE	T	6
SE	CRPT1	6
SE	CRPT2	6
SE	CRT	6
SE	N/CRPT1	6
SE	CRPT1/N	6
CB	N	6
CB	T	6
CB	CRPT1	6
CB	CRPT2	6
CB	CRT	6
G 109	N	6
G 109	T	6
G 109	CRPT1	6
G 109	CRPT2	6
G 109	CRT	6

2.5   Mechanical Tests

Tension tests were performed on the microalloyed steels to determine whether their composition affects their mechanical properties. Results include tensile strength, yield strength, and percent elongation. CRPT1, CRPT2, and CRT do not have a well-defined yield plateau so their yield strengths were determined from the stress-strain diagram based on 0.5% strain. Bend tests were also performed to evaluate the ductility of the steels.

Chapter 3

Results

This chapter presents the results obtained in the corrosion potential, macrocell, Southern Exposure, cracked beam, and ASTM G 109 tests. The tests cover the two conventional (N and T) and three microalloyed steels (CRPT1, CRPT2, and CRT) described in Chapter 2. Mechanical properties, including yield and tensile strengths, elongation, and the results of the bend tests are also presented for T, CRPT1, CRPT2 and CRT steels.

Results from the corrosion potential test demonstrate that the five different steels have a similar tendency to corrode, while the macrocell test results show no advantage to the microalloyed steels over the conventional steels. The more realistic bench-scale tests show a relatively consistent advantage for CRT steel (11%, 4%, and 64% less total corrosion loss than N steel for the SE, CB and G 109 tests, respectively), although the advantage is smaller in the SE and CB tests than observed for one of the microalloyed steels in a previous study (Darwin 1995), which consistently exhibited one-half the corrosion rate of conventional steel in the bench-scale tests.

3.1   Rapid Evaluation Tests

3.1.1   Corrosion Potential Test

Average corrosion potential results are shown in Table 3.1 and Figures 3.1 to 3.3. The tests cover bare bars in 1.6 m ion NaCl and simulated concrete pore solution, and mortar-embedded bars in 0.4 and 1.6 m ion NaCl and simulated concrete pore solution. Table 3.1 lists the average corrosion potentials with respect to a saturated calomel electrode on the last day of the testing period (day 40). Results for individual specimens are given in the Appendix (Figures

40

A.1 to A.15). The more negative the corrosion potential, the greater the likelihood of corrosion. As presented in Table 1.2, when the corrosion potential versus the saturated calomel electrode is more negative than –0.275 V, there is greater than 90% probability that corrosion is occurring; when the potential is more positive than –0.125 V, there is greater than 90% probability that corrosion is not occurring; and when the potential is between   –0.125 and –0.275 V, it is uncertain if corrosion is occurring (ASTM C 876).

TABLE 3.1: Corrosion Potential in Volts versus Saturated Calomel Electrode on Day 40

Steel Designation	Specimen					Average	Std. Deviation
	1	2	3	4	5		
Bare bars in 1.6 m ion NaCl							
N	-0.522	-0.261	-0.529	-0.518	-0.446	-0.455	0.114
T	-0.536	-0.541	-0.525	-0.526	-0.564	-0.538	0.016
CRPT1	-0.541	-0.501	-0.482	-0.501	-0.507	-0.506	0.022
CRPT2	-0.528	-0.509	-0.453	-0.521	-0.523	-0.507	0.031
CRT	-0.567	-0.579	-0.576	-0.519	-0.551	-0.558	0.025
Mortar-embedded bars in 0.4 m ion NaCl							
N	-0.545	-0.470	-0.469	-	-	-0.495	0.044
T	-0.517	-0.412	-0.470	-	-	-0.466	0.053
CRPT1	-0.424	-0.412	-0.490	-	-	-0.442	0.042
CRPT2	-0.495	-0.570	-0.572	-	-	-0.546	0.044
CRT	-0.452	-0.461	-0.405	-	-	-0.439	0.030
Mortar-embedded bars in 1.6 m ion NaCl							
N	-0.520	-0.487	-0.375	-	-	-0.461	0.076
T	-0.521	-0.284	-0.420	-	-	-0.408	0.119
CRPT1	-0.530	-0.520	-0.529	-	-	-0.526	0.006
CRPT2	-0.533	-0.511	-0.131	-	-	-0.392	0.226
CRT	-0.393	-0.280	-0.467	-	-	-0.380	0.094

Results from the corrosion potential test indicate that the five different steels have a similar tendency to corrode. After the end of the test period, all steels, either bare or embedded in mortar, have an average corrosion potential that is more negative than -0.275 V, which indicates a high probability that corrosion is occurring. Table 3.1 shows that for bare specimens, N steel has the lowest tendency to corrode while CRT steel had the highest tendency to corrode. For bars embedded in mortar in 0.4 m ion NaCl solution, CRT and CRPT1 have the lowest tendency to corrode while CRPT2 has the highest tendency to corrode. Finally, for bars embedded in

mortar, in 1.6 m ion NaCl solution, CRT has the lowest tendency to corrode, while CRPT1 has the highest tendency to corrode.

Figure 3.1 shows the average corrosion potential with respect to a saturated calomel electrode for bare bars in 1.6 m ion NaCl and simulated concrete pore solution. Figures A.1 to A.5 show the results for the individual specimens. At the initial reading, all average potential readings are below –0.300 V, and after two days all readings are below –0.400 V, indicating that the steels have a high tendency to corrode. The potential continues to decrease slightly with time, reaching values between –0.450 and –0.550 V at day 40. Through most of the testing period the conventional steels, N and T, show the most positive potentials, although the potential of T steel becomes more negative in the last 7 days. CRPT1 and CRT steel show the most negative corrosion potentials through most of the testing period. At the end of the 40-day test period, N had the most positive corrosion potential with –0.455 V, followed by CRPT1 with –0.506 V, CRPT2 with –0.507 V, T with –0.538 V, and CRT with –0.558 V.
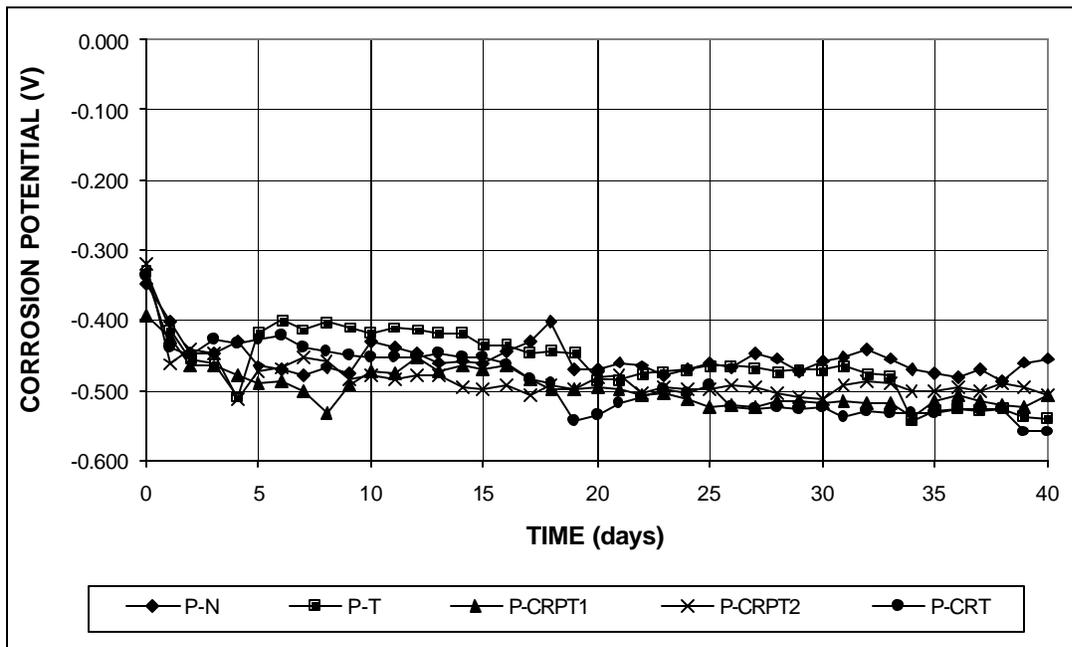
FIGURE 3.1: Average Corrosion Potential versus Saturated Calomel Electrode, Bare Bars in 1.6 m Ion NaCl and Simulated Concrete Pore Solution

Figure 3.2 shows the average corrosion potential with respect to a saturated calomel electrode for bars embedded in mortar in 0.4 m ion NaCl and simulated concrete pore solution. Figures A.6 to A.10 show the results for the individual specimens. All of the average readings on the first day were close to –0.200 V; they gradually decreased to values between –0.400 to –0.500 V by day 8, where they remained for the balance of the test. Through most of the testing period CRPT2 had the most positive corrosion potential, around –0.400 V, while N steel had the most negative corrosion potential, around –0.500 V, with the other steels exhibiting intermediate values. At day 37, the corrosion potential of CRPT2 steel became more negative and went from a value of –0.400 V, which had been maintained through most of the test period, to a value of –0.440V, ultimately dropping below –0.500 V by the end of the test. At the end of the 40-day test period, CRT had the most positive corrosion potential with –0.439 V, followed by CRPT1 with –0.442 V, T with –0.446 V, N with –0.495 V, and CRPT2 with –0.546 V.
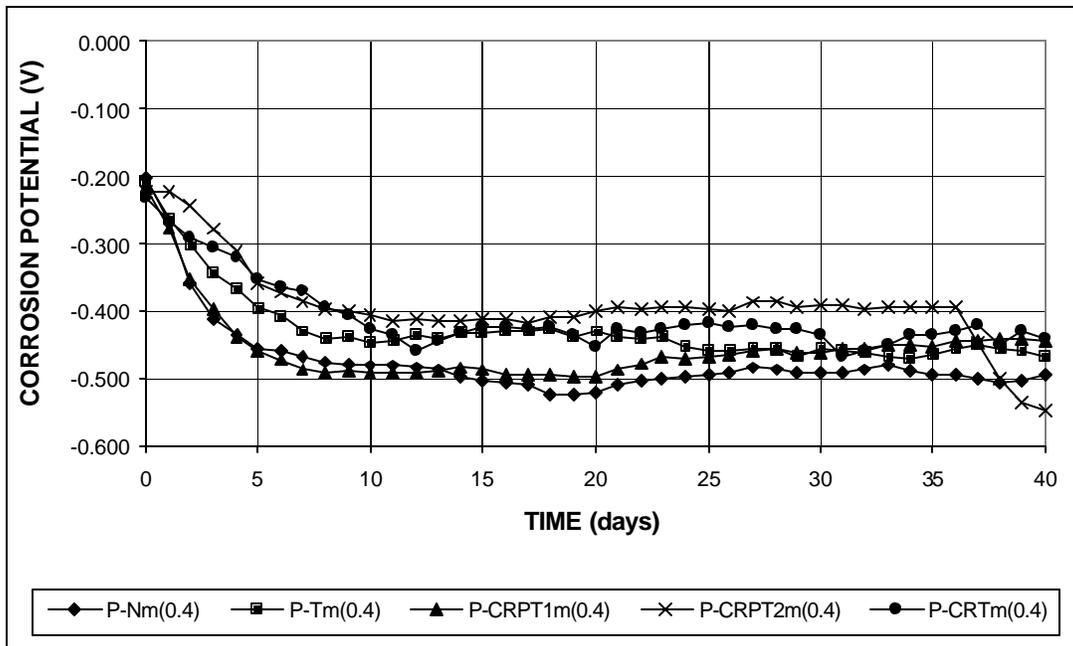
FIGURE 3.2: Average Corrosion Potential versus Saturated Calomel Electrode, Mortar-Embedded Bars in 0.4 m Ion NaCl and Simulated Concrete Pore Solution

Figure 3.3 shows the average corrosion potential with respect to a saturated calomel electrode for bars embedded in mortar in 1.6 m ion NaCl and simulated concrete pore solution. Figures A.11 to A.15 show the results for the individual specimens. The average readings on the first day were between –0.200 and –0.300 V for the five types of steel. The corrosion potential gradually became more negative, and by Day 8, the average corrosion potential for N and CRPT2 steels was about –0.350 V, while for T, CRPT1 and CRT steel it was about –0.500 V. The potential for CRPT1 steel continued to become more negative and reached a value of about –0.525 V for the rest of the testing period. After day 8, the average corrosion potential of CRT and T steel increased to values of approximately –0.400 V, while the average corrosion potential of N and CRPT1 steel decreased to a value of approximately –0.400 V. After day 34 the corrosion potential of N steel dropped to –0.450 V. At the end of the 40-day test, CRT had the most positive corrosion potential with –0.380 V, followed by CRPT2 with –0.392 V, T with –0.408 V, N with –0.461 V, and CRPT1 with –0.526 V.
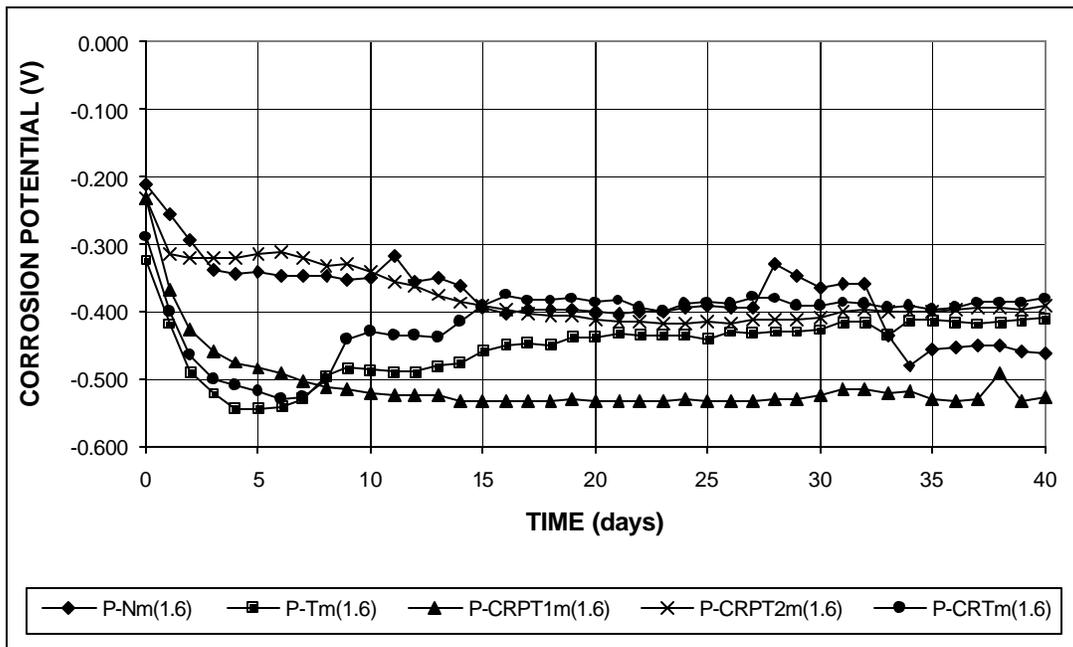

FIGURE 3.3: Average Corrosion Potential versus Saturated Calomel Electrode, Mortar-Embedded Bars in 1.6 m Ion NaCl and Simulated Concrete Pore Solution

44

3.1.2 Corrosion Macrocell Test

Average corrosion rate results are shown in Table 3.2 and Figures 3.4 to 3.8. Table 3.2 lists the average corrosion rates on the last day of the testing period (day 100). Figures with the results for the individual specimens are given in the Appendix (Figures A.16 to A.40). The tests cover bare bars in 1.6 m ion NaCl and simulated concrete pore solution, and mortar-embedded bars in 0.4 and 1.6 m ion NaCl and simulated concrete pore solution. Mortar specimens include bars with the ends protected with an epoxy-filled cap and bars without caps on the ends.

The results from the macrocell tests show no improved corrosion performance for the microalloyed steels when compared to the conventional steels. Table 3.2 shows that for bare bars, T steel had the lowest corrosion rate in the last day of testing, while CRPT2 has the highest corrosion rate. For the different tests with bars embedded in mortar, the lowest corrosion rate corresponds to conventional steel.

TABLE 3.2: Corrosion Rate in mm/Year on Day 100 as Measured in the Macrocell Test

Steel Designation	Specimen					Average	Std. Deviation
	1	2	3	4	5		
Bare bars in 1.6 m ion NaCl							
N	54.59	56.17	12.28	37.20	40.79	40.21	17.68
T	48.52	26.57	26.10	8.35	42.06	30.32	15.68
CRPT1	26.27	37.52	64.70	21.51	37.09	37.42	16.75
CRPT2	45.77	77.69	26.10	53.67	43.93	49.43	18.74
CRT	74.56	42.08	35.94	44.01	27.60	44.84	17.81
Mortar-embedded bars with caps in 0.4 m ion NaCl							
N	1.32	1.11	0.71	0.71	-	0.96	0.30
T	4.12	0.59	0.87	1.70	-	1.82	1.60
CRPT1	2.89	0.52	0.00	0.95	-	1.09	1.26
CRPT2	1.58	0.40	4.24	1.47	-	1.92	1.64
CRT	1.47	0.27	0.16	3.03	-	1.23	1.34
Mortar-embedded bars with caps in 1.6 m ion NaCl							
N	3.47	3.80	0.63	5.43	-	3.33	2.00
T	3.72	3.41	2.94	1.00	-	2.77	1.22
CRPT1	4.37	7.66	5.04	3.05	-	5.03	1.94
CRPT2	5.66	2.66	4.02	3.49	-	3.96	1.26
CRT	4.46	4.79	3.84	9.41	-	5.62	2.55
Mortar-embedded bars without caps in 0.4 m ion NaCl							
N	3.17	0.45	2.28	1.40	0.16	1.49	1.25
T	0.78	0.74	1.00	0.00	1.00	0.70	0.41
CRPT1	1.73	2.09	1.82	0.42	1.47	1.51	0.65
CRPT2	2.16	1.64	1.82	0.20	0.16	1.20	0.95
CRT	1.57	2.18	0.00	0.45	0.92	1.02	0.87
Mortar-embedded bars without caps in 1.6 m ion NaCl							
N	3.59	2.49	2.27	0.67	2.21	2.25	1.04
T	4.65	3.41	2.81	3.85	1.03	3.15	1.36
CRPT1	6.56	3.21	2.86	0.35	4.21	3.44	2.25
CRPT2	3.68	2.76	4.95	3.81	0.93	3.23	1.50
CRT	3.49	4.73	3.61	0.64	2.66	3.03	1.53

Figure 3.4 shows the average corrosion rate for bare bars in 1.6 m ion NaCl and simulated concrete pore solution. Figures A.16 to A.20 show the results for the individual specimens. The average corrosion rates on day 0 rangd from 0.1 to 13.7 μm/year, and by day 2 all types of steel showed corrosion rates above 25 μm/year. The corrosion rate gradually increased for all steel types until it reached a maximum (ranging from 30 to 55 μm/year) between days 10 and 20; it then began to slowly decrease. CRPT1, CRPT1, and CRT steels had the highest corrosion rate for the first 45 days. For most of the testing period, T steel showed the lowest corrosion rate, although at day 79 its corrosion rate increased, and for the last 21 days, T steel had a corrosion rate that was similar to that of CRPT1 and CRT steels. The corrosion rate

46

of CRT steel was similar to that of T steel for the first 45 days, but increased thereafter. As shown in Table 3.2, at the end of the test period, T steel has the lowest average corrosion rate with 30.32 µm/year, followed by CRPT1 with 37.42 µm/year, N with 40.21 µm/year, CRPT with 44.84 µm/year, and CRPT2 with 49.43 µm/year.

Figure 3.5 shows the average corrosion rate for bars with epoxy-filled caps on the ends, embedded in mortar, in 0.4 m ion NaCl and simulated concrete pore solution. Figures A.21 to A.25 show the results for the individual specimens. Average corrosion rates for most of the test period ranged from 0.50 µm/year for N steel to 2.5 µm/year for CRPT2 steel. The rest of the steels had intermediate values, ranging from 1.0 to 1.75 µm/year. As shown in Table 3.2, at the end of the test period, N steel has the lowest average corrosion rate with 0.96 µm/year, followed by CRPT1 with 1.09 µm/year, CRT with 1.23 µm/year, T with 1.82 µm/year, and CRPT2 with 1.92 µm/year.
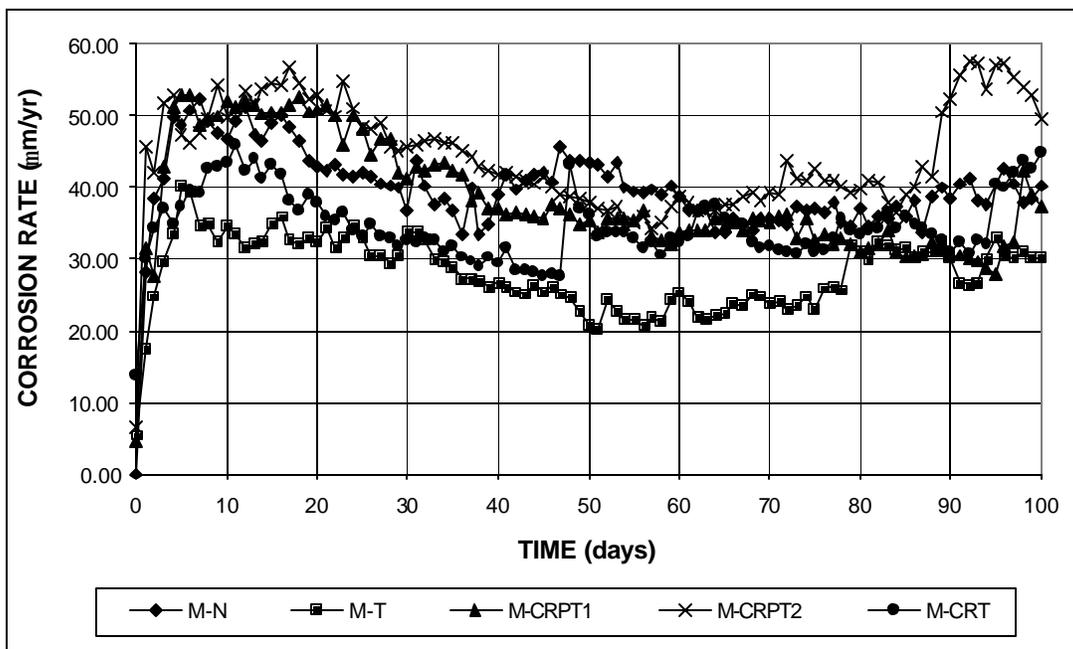
FIGURE 3.4: Macrocell Test – Average Corrosion Rate, Bare Bars in 1.6 m Ion NaCl and Simulated Concrete Pore Solution

47
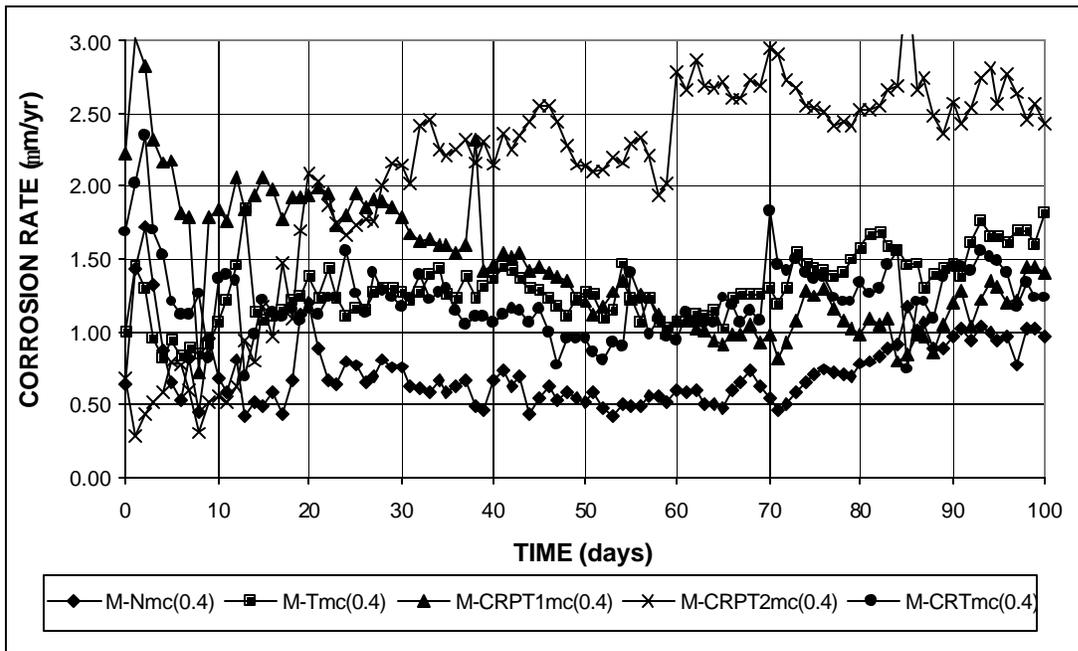
FIGURE 3.5: Macrocell Test – Average Corrosion Rate, Mortar-Embedded Bars with Epoxy-Filled Caps on the End, in 0.4 m Ion NaCl and Simulated Concrete Pore Solution

Figure 3.6 shows the average corrosion rate for bars with epoxy-filled caps on the ends, embedded in mortar in 1.6 m ion NaCl and simulated concrete pore solution. Figures A.26 to A.30 show the results for the individual specimens. After week 20, all steels showed relatively constant average corrosion rates, ranging from 2 to 4 μm/year. Conventional Thermex (T) steel exhibited a constant corrosion rate of approximately 2 μm/year for most of the testing period, which is significantly lower than other steels, which showed corrosion rates above 3 μm/year for most of the testing period. CRPT1 steel showed consistently higher corrosion rate than the other steels in this test, with N steel also showing a higher corrosion rate for the first 50 days. CRT steel showed a corrosion rate of approximately 3.0 μm/year until day 68, after which it increased with time for the rest of the testing period, reaching values greater than 4.0 μm/year after day 73 and greater than 5.0 μm/year after day 91. The jumps in the average corrosion rate observed at

48

days 73 and 91 for CRT are caused by very high corrosion rates for one of the four individual specimens, as shown in Figure A.29. As shown in Table 3.2, at the end of the test period, T steel has the lowest average corrosion rate with 2.77 µm/year, followed by N with 3.33 µm/year, CRPT2 with 3.96 µm/year, CRPT1 with 5.03 µm/year, and CRT with 5.63 µm/year.
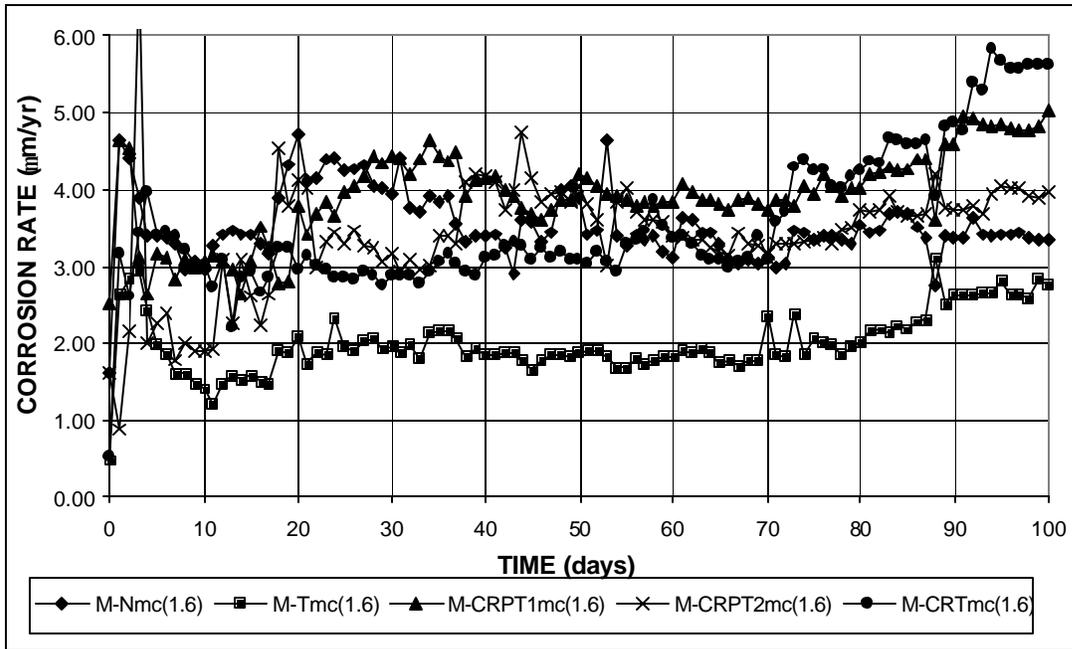
FIGURE 3.6: Macrocell Test – Average Corrosion Rate, Mortar-Embedded Bars with Epoxy-Filled Caps on the End, in 1.6 m Ion NaCl and Simulated Concrete Pore Solution

Figure 3.7 shows the average corrosion rate for bars embedded in mortar, without caps on the ends, in 0.4 m ion NaCl and simulated concrete pore solution. Figures A.31 to A.35 show the results for the individual specimens. The average corrosion rates ranged from 0.50 to 2.00 µm/year, with T steel showing a slightly lower corrosion rate than the rest of the bars during most of the testing period. N and CRPT1 steels showed the highest corrosion rates during most of the testing period. As shown in Table 3.2, at the end of the test period, T steel had the lowest average corrosion rate with 0.70 µm/year, followed by CRT with 1.02 µm/year, CRPT2 with 1.20 µm/year, N with 1.49 µm/year, and CRPT1 with 1.51 µm/year.
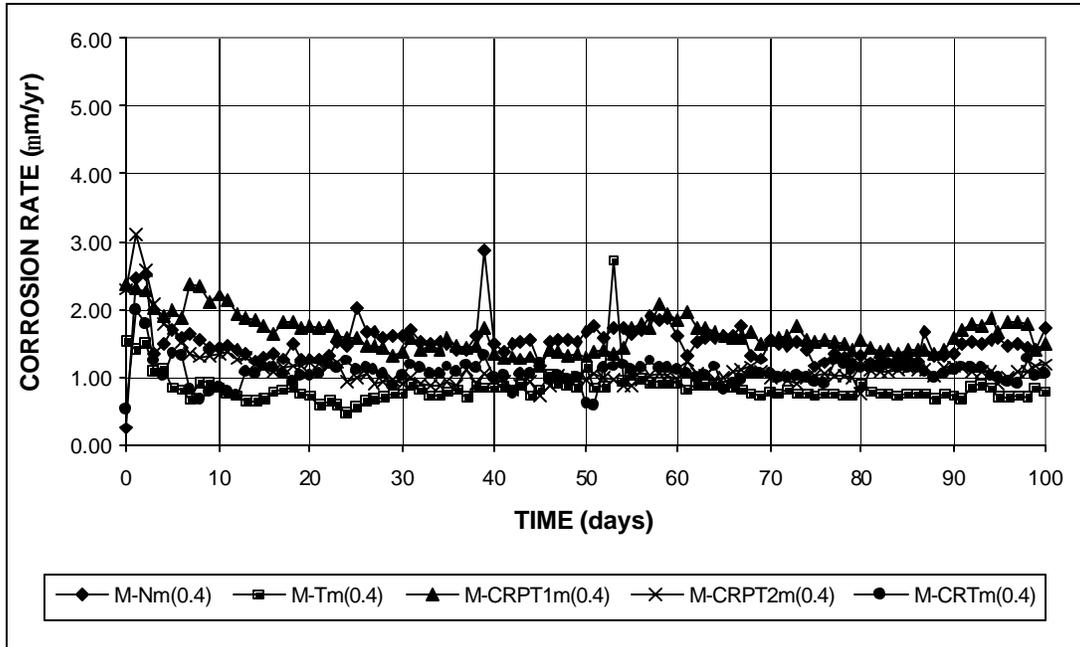
49

FIGURE 3.7: Macrocell Test – Average Corrosion Rate, Mortar-Embedded Bars without Cap on the End, in 0.4 m Ion NaCl and Simulated Concrete Pore Solution

Figure 3.8 shows the average corrosion rate for bars embedded in mortar, without caps on the ends, in 1.6 m ion NaCl and simulated concrete pore solution. The corrosion rates range from 2 to 5 µm/year. Figures A.36 to A.40 show the results for the individual specimens. The lowest average corrosion rate corresponded to N steel. CRPT2 and CRT had the highest average corrosion rates for most of the test period, although the corrosion rate for CRPT1 steel increased during the last 15 weeks to values of approximately 1.75 µm/year. As shown in Table 3.2, at the end of the test period, N steel had the lowest average corrosion rate with 2.25 µm/year, followed by CRT with 3.03 µm/year, T with 3.15 µm/year, CRPT2 with 3.23 µm/year, and CRPT1 with 3.44 µm/year.
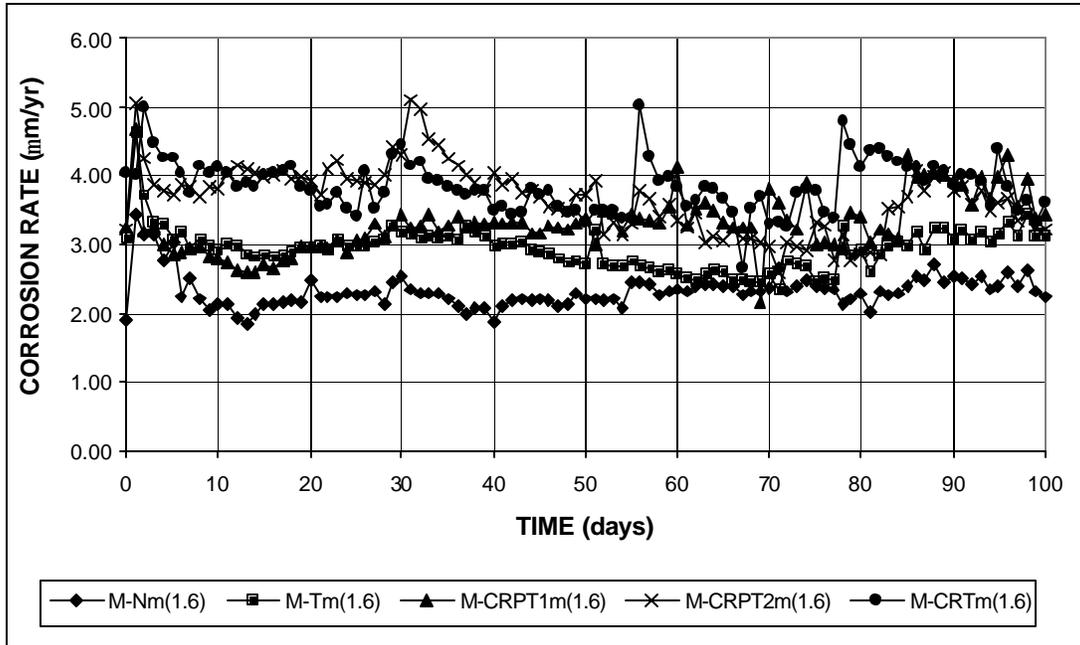
FIGURE 3.8: Macrocell Test – Average Corrosion Rate, Mortar-Embedded Bars without Cap on the End, in 1.6 m Ion NaCl and Simulated Concrete Pore Solution

3.2   Bench-Scale Tests

Results from the bench-scale tests include the corrosion rate, total corrosion loss, corrosion

potential of top and bottom mats, and mat-to-mat resistance. Corrosion potential readings on the

bench-scale tests are reported versus the copper-copper sulfate electrode. As presented in Table

1.2, when the corrosion potential versus a copper-copper sulfate electrode is more negative than

–0.350 V, there is greater than 90% probability that corrosion is occurring; when the potential is

more positive than –0.200 V, there is greater than 90% probability that corrosion is not

occurring; and when the potential is between –0.200 and –0.350 V, it is uncertain if corrosion is

occurring (ASTM C 876).

Tables 3.3 to 3.8 summarize the average values for six specimens for each type of steel at

week 70 of the 96-week testing period. Week 70 was chosen as the cutoff point for reporting

results because some individual specimens in the Southern Exposure and cracked beam tests

exhibited unusual behavior after this period, which affected the average results. This behavior

51

included specimens with extremely high corrosion rates when compared to the other individual specimens in the same set, and specimens that showed drops in corrosion rate as a result of more negative potentials in the bottom mat of steel, which indicates that chlorides have reached the bottom steel. Figures 3.9 to 3.15 show the average readings for the full testing period. Results for the individual specimens are shown in Figures A.41 to A.75. Besides tests for the five steels, Southern Exposure test results also include specimens with a combination of conventional and microalloyed steels. CRPT1 steel was chosen as the microalloyed steel used for these tests because initial results from the Southern Exposure tests (Figure 3.9) indicated better corrosion performance of this steel when compared to the other two microalloyed steels.

TABLE 3.3: Corrosion Rate in mm/Year at Week 70 as Measured in the Bench-Scale Tests

Steel Designation	Specimen						Average	Std. Deviation
	1	2	3	4	5	6		
Southern Exposure								
N	8.41	0.73	3.41	2.33	3.80	5.76	4.07	2.70
T	10.70	2.44	4.98	32.63	1.30	6.51	9.76	11.68
CRPT1	4.36	1.30	10.06	6.94	0.05	2.13	4.14	3.79
CRPT2	7.56	4.90	13.28	7.20	3.41	2.25	6.43	3.94
CRT	3.78	6.96	6.70	1.46	5.03	0.91	4.14	2.57
N/CRPT1	3.75	9.58	9.54	4.39	6.47	6.18	6.65	2.48
CRPT1/N	9.58	0.21	5.06	4.56	3.71	6.61	4.96	3.11
Cracked Beam								
N	9.55	4.55	2.22	3.92	17.61	6.22	7.34	5.61
T	9.43	3.14	2.27	9.85	4.16	1.57	5.07	3.65
CRPT1	2.41	1.50	1.00	6.88	12.27	4.93	4.83	4.27
CRPT2	1.54	1.64	0.56	9.61	1.76	9.39	4.08	4.22
CRT	1.30	4.64	0.00	5.99	9.81	3.30	4.17	3.51
ASTM G 109								
N	3.37	0.99	1.21	0.00	9.642	7.607	3.80	3.94
T	0.00	0.00	2.13	8.30	4.587	2.066	2.85	3.16
CRPT1	1.48	1.91	0.00	10.72	4.508	4.881	3.92	3.82
CRPT2	1.92	2.70	2.68	11.15	1.979	0.000	3.40	3.92
CRT	2.08	1.96	0.50	6.90	2.426	4.173	3.01	2.24

TABLE 3.4: Total Corrosion Loss in mm at Week 70 as Measured in the Bench-Scale Tests

Steel Designation	Specimen						Average	Std. Deviation
	1	2	3	4	5	6		
Southern Exposure								
N	7.13	8.89	6.90	3.02	4.19	4.56	5.78	2.21
T	11.50	4.92	5.35	5.15	0.93	7.66	5.92	3.49
CRPT1	3.96	3.15	7.95	7.90	1.43	1.64	4.34	2.94
CRPT2	8.22	4.56	13.06	6.95	4.79	1.40	6.50	3.97
CRT	8.31	7.45	7.68	1.39	5.09	1.14	5.18	3.22
N/CRPT1	6.00	3.92	4.72	7.62	7.95	8.45	6.44	1.85
CRPT1/N	6.05	6.00	2.84	4.46	9.14	11.58	6.68	3.18
Cracked Beam								
N	10.36	7.75	4.98	8.57	7.61	5.78	7.51	1.93
T	9.59	7.42	8.86	10.96	10.48	4.99	8.72	2.21
CRPT1	9.08	5.80	5.17	12.34	9.67	6.97	8.17	2.70
CRPT2	7.20	5.96	4.14	13.04	5.79	8.88	7.50	3.14
CRT	5.57	8.52	5.47	8.09	8.29	7.47	7.24	1.37
ASTM G 109								
N	2.92	1.45	1.03	3.05	4.190	3.007	2.61	1.17
T	0.01	0.00	0.34	6.71	0.687	1.839	1.60	2.60
CRPT1	0.38	0.34	0.01	6.82	2.073	3.084	2.12	2.59
CRPT2	0.46	0.51	0.94	8.95	1.377	0.041	2.05	3.41
CRT	0.65	0.21	0.01	1.77	1.853	1.138	0.94	0.78

TABLE 3.5: Mat-to-Mat Resistance in ohms at Week 1 as Measured in the Bench-Scale Tests

Steel Designation	Specimen						Average	Std. Deviation
	1	2	3	4	5	6		
Southern Exposure								
N	-	-	-	158	147	139	148	10
T	-	-	-	154	176	119	150	29
CRPT1	-	-	-	150	174	124	149	25
CRPT2	-	-	-	144	131	123	133	11
CRT	-	-	-	164	131	136	144	18
N/CRPT1	111	150	149	124	120	121	129	16
CRPT1/N	116	113	152	130	122	125	126	14
Cracked Beam								
N	327	341	358	297	306	323	325	22
T	288	306	253	196	206	229	246	44
CRPT1	272	312	305	189	190	305	262	58
CRPT2	293	274	331	199	224	279	267	48
CRT	304	286	347	197	218	291	274	56
ASTM G 109								
N	158	168	163	145	143	138	159	10
T	327	325	20	139	128	155	182	121
CRPT1	320	-	261	144	148	158	206	80
CRPT2	312	222	255	138	155	159	207	68
CRT	316	229	270	130	164	164	212	72

TABLE 3.6: Mat-to-Mat Resistance in ohms at Week 70 as Measured in the Bench-Scale Tests

Steel Designation	Specimen 1	2	3	4	5	6	Average	Std. Deviation
Southern Exposure								
N	514	362	1035	1509	1201	824	908	430
T	411	1390	833	523	6461	448	1678	2372
CRPT1	680	1985	359	400	6727	656	1801	2486
CRPT2	211	1234	280	580	890	2640	973	902
CRT	206	698	445	1659	563	2720	1048	959
N/CRPT1	390	466	497	405	377	377	419	51
CRPT1/N	339	1216	758	586	556	458	652	309
Cracked Beam								
N	909	2026	3603				2179	1354
T	581	1741	2904	641	1198	5455	2087	1859
CRPT1	3679	2369	3089	630	446	1818	2005	1301
CRPT2	4288	3402	1028	673	3938	918	2375	1673
CRT	1628	1564	3980	1578	487	2678	1986	1198
ASTM G 109								
N	632	1528	1690	563	484	536	906	549
T	1509	1135	1548	350	665	2086	1216	635
CRPT1	1420	1634	740	359	641	895	948	486
CRPT2	1301	1362	965	579	1815	734	1126	456
CRT	1196	1425	997	634	1619	827	1116	370

TABLE 3.7: Corrosion Potential of Top Mat in Volts versus Copper-Copper Sulfate Electrode at Week 70 as Measured in the Bench-Scale Tests

Steel Designation	Specimen 1	2	3	4	5	6	Average	Std. Deviation
Southern Exposure								
N	-0.536	-0.503	-0.587	-0.592	-0.606	-0.618	-0.574	0.045
T	-0.627	-0.596	-0.618	-0.627	-0.492	-0.615	-0.596	0.052
CRPT1	-0.601	-0.603	-0.578	-0.597	-0.459	-0.606	-0.574	0.057
CRPT2	-0.611	-0.594	-0.588	-0.621	-0.617	-0.600	-0.605	0.013
CRT	-0.595	-0.610	-0.573	-0.512	-0.606	-0.580	-0.579	0.036
N/CRPT1	-0.529	-0.525	-0.587	-0.550	-0.392	-0.412	-0.499	0.079
CRPT1/N	-0.584	-0.599	-0.652	-0.402	-0.412	-0.478	-0.521	0.105
Cracked Beam								
N	-0.620	-0.576	-0.640	-0.516	-0.626	-0.639	-0.603	0.049
T	-0.666	-0.653	-0.640	-0.656	-0.614	-0.428	-0.610	0.091
CRPT1	-0.646	-0.625	-0.598	-0.619	-0.671	-0.590	-0.625	0.030
CRPT2	-0.629	-0.645	-0.581	-0.638	-0.378	-0.644	-0.586	0.105
CRT	-0.611	-0.603	-0.591	-0.623	-0.392	-0.655	-0.579	0.094
ASTM G 109								
N	-0.479	-0.512	-0.535	-0.475	-0.556	-0.536	-0.516	0.033
T	-0.112	-0.164	-0.405	-0.532	-0.502	-0.526	-0.374	0.189
CRPT1	-0.423	-0.407	-0.090	-0.514	-0.514	-0.515	-0.411	0.164
CRPT2	-0.410	-0.416	-0.446	-0.530	-0.519	-0.133	-0.409	0.144
CRT	-0.426	-0.387	-0.328	-0.541	-0.517	-0.516	-0.453	0.085

TABLE 3.8: Corrosion Potential of Bottom Mat in Volts versus Copper-Copper Sulfate Electrode at Week 70 as Measured in the Bench-Scale Tests

Steel Designation	Specimen						Average	Std. Deviation
	1	2	3	4	5	6		
Southern Exposure								
N	-0.344	-0.453	-0.242	-0.327	-0.346	-0.375	-0.348	0.068
T	-0.399	-0.400	-0.437	-0.196	-0.186	-0.383	-0.334	0.112
CRPT1	-0.444	-0.552	-0.404	-0.244	-0.232	-0.306	-0.364	0.125
CRPT2	-0.541	-0.280	-0.349	-0.212	-0.341	-0.247	-0.328	0.117
CRT	-0.560	-0.378	-0.237	-0.234	-0.256	-0.365	-0.338	0.126
N/CRPT1	-0.254	-0.353	-0.349	-0.323	-0.233	-0.225	-0.290	0.059
CRPT1/N	-0.246	-0.186	-0.283	-0.208	-0.184	-0.240	-0.225	0.039
Cracked Beam								
N	-0.468	-0.280	-0.328	-0.562	-0.378	-0.505	-0.420	0.109
T	-0.545	-0.262	-0.369	-0.252	-0.431	-0.252	-0.352	0.120
CRPT1	-0.174	-0.344	-0.287	-0.365	-0.459	-0.311	-0.323	0.094
CRPT2	-0.358	-0.418	-0.291	-0.315	-0.208	-0.352	-0.324	0.071
CRT	-0.313	-0.255	-0.257	-0.440	-0.177	-0.359	-0.300	0.092
ASTM G 109								
N	-0.420	-0.280	-0.281	-0.485	-0.210	-0.225	-0.317	0.111
T	-0.105	-0.225	-0.191	-0.218	-0.229	-0.256	-0.204	0.053
CRPT1	-0.174	-0.172	-0.162	-0.205	-0.249	-0.229	-0.199	0.035
CRPT2	-0.162	-0.186	-0.167	-0.231	-0.245	-0.132	-0.187	0.043
CRT	-0.237	-0.178	-0.162	-0.246	-0.237	-0.224	-0.214	0.035

3.2.1 Southern Exposure Test

As shown in Table 3.3, at week 70 N, CRPT1, and CRT steels had the lowest average corrosion rates (4.07 µm/year for N steel and 4.14 µm/year for CRPT1 and CRT), while T steel had the highest corrosion rate (9.76 µm/year). CRPT2 steel, as well as the specimens with a combination of N and CRPT1 steels had intermediate corrosion rates, ranging from 4.96 to 6.65 µm/year. The average total corrosion loss shown in Table 3.4 indicates that, after 70 weeks, CRPT1 and CRT steels had the lowest corrosion loss with 4.34 µm and 5.18, respectively. This corresponds to 25% and 11% less than N steel, which had a corrosion loss of 5.78 µm. CRPT2 had the highest corrosion loss with 6.50 µm, 12% higher than N steel. Mat-to-mat resistance for all specimens has between 126 and 150 ohms after 1 week, and increased to values between 419 and 1801 by week 70. The increase in the mat-to-mat resistance has a result of the deposition of corrosion products on the surface of and in the region surrounding the reinforcing bars. Average corrosion potential of the top mat for all steels has more negative than –0.499 V, which indicates

a high tendency to corrode. Average corrosion potential of the bottom mat ranges from –0.225 to –0.364 V, which indicates a lower probability of corrosion.

Figure 3.9 shows that the corrosion rates start increasing after the first week for all steels and reached values between approximately 4 and 8 µm/year after 30 weeks, after which the corrosion rates remained relatively constant. After week 80 the corrosion rates dropped slightly. CRPT1 had a slightly lower corrosion rate than the rest of the steels for the first 50 weeks of the testing period. The corrosion rate for T steel jumped to values as high as 15 µm/year after week 70, after which it remained at 14 µm/year for 9 weeks and then dropped to around 10 µm/year for the last weeks of testing. This jump in the average has the result of extremely high corrosion rates in one of the specimens, as shown in Figure A.42. The corrosion rate of CRT dropped below the rest of the steels during the last two weeks.
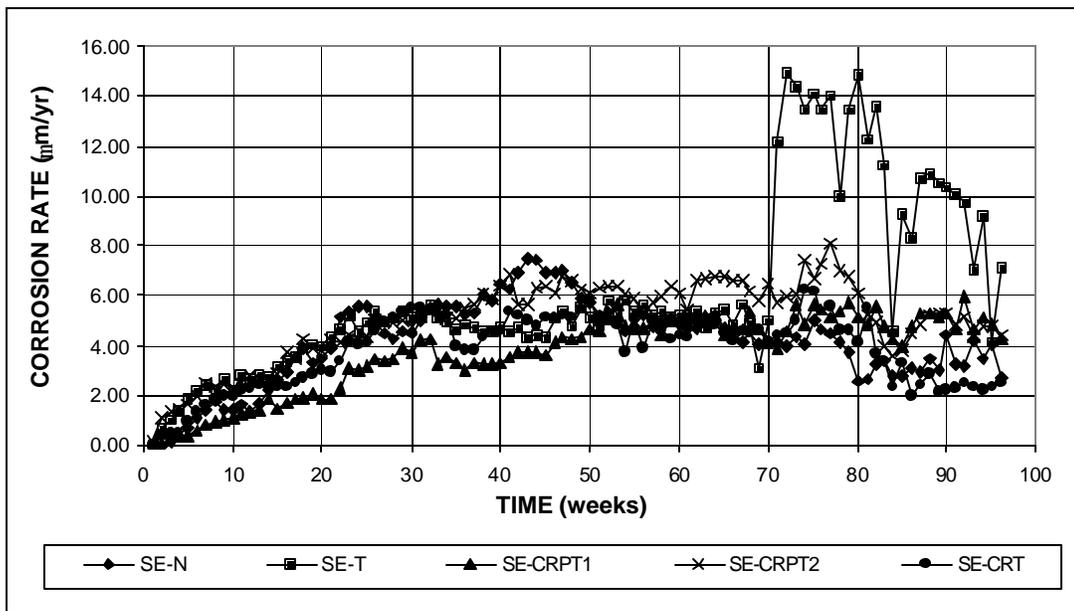
FIGURE 3.9: Southern Exposure Test – Average Corrosion Rate

Figure 3.10 shows the corrosion rate for specimens with mixed steel. Figures A.48 to A.49 show the results for the individual specimens. Specimens with N steel in the top mat have the same behavior as those with CRPT1 on the top mat. Although the specimens with N steel on

56

the top mat start corroding later than the other specimens, after week 10, both show very similar

corrosion rates for the rest of the testing period. The average corrosion rate increased with time

and reached a maximum value between 8 and 10 µm/year at week 32. The corrosion rates remain

in the range of 6 to 8 µm/year from week 34 to week 60, after which the values started to drop.

At the end of the testing period, corrosion rates for both types of specimens are around 5

µm/year.
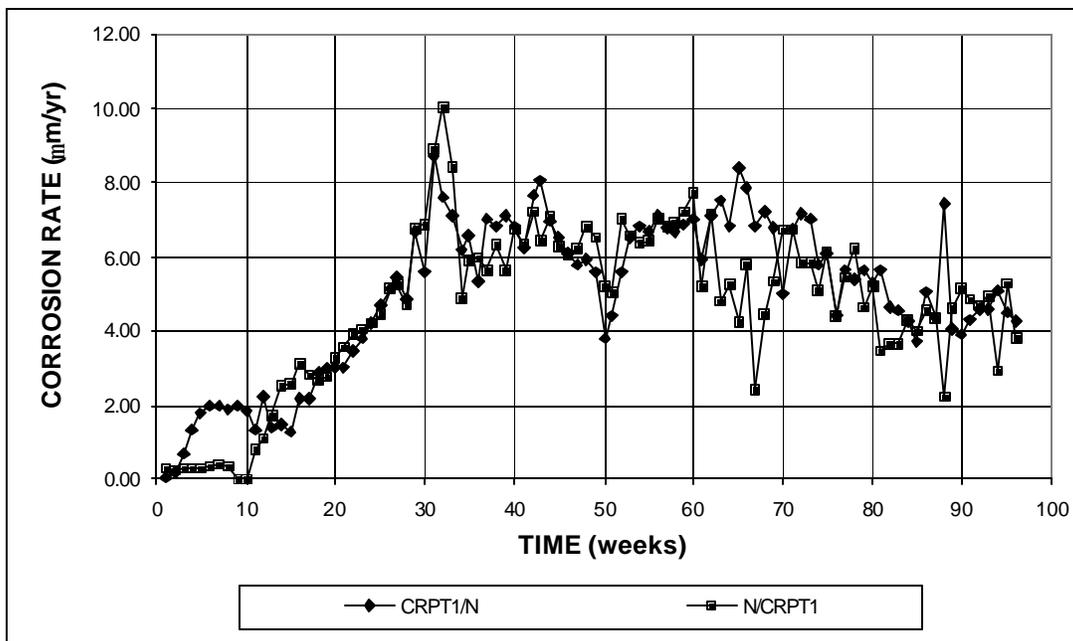
**FIGURE 3.10: Southern Exposure Test – Average Corrosion Rate,
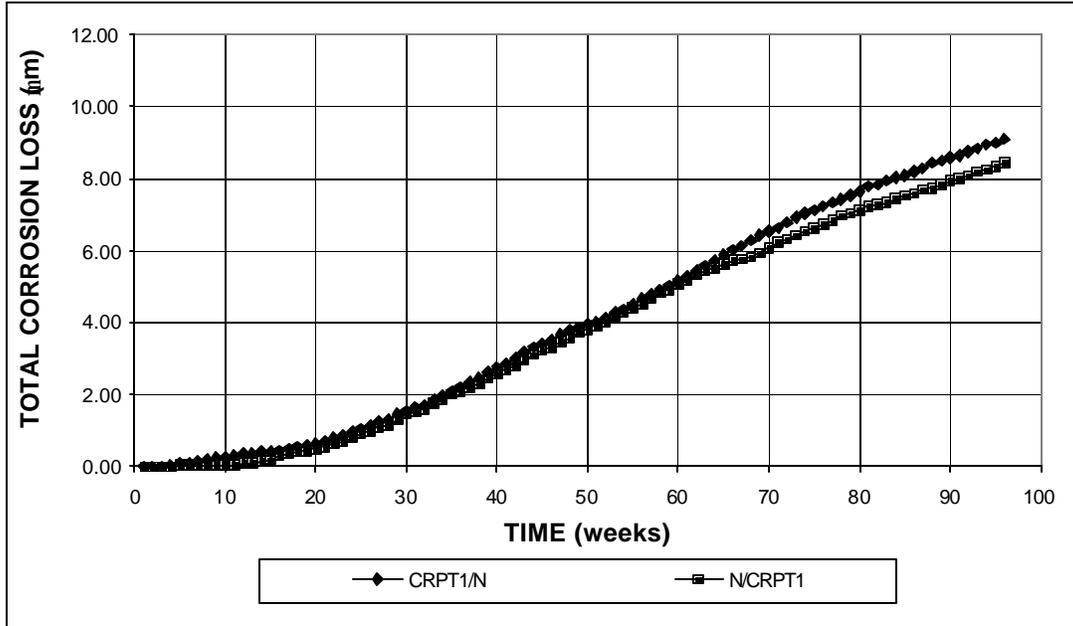Specimens with Mixed Steel**

Figure 3.11 shows the total corrosion loss for the SE tests. Figures A.49 to A.53 show the

results for the individual specimens. During the first 35 weeks, the slope of the curves increased

with time, as the corrosion rate increased. For the first 10 weeks all steels show similar total

corrosion loss. After week 10, CRPT1 began to show a lower corrosion loss than the rest of the

steels and the difference increased slightly with time. After week 60, CRPT2 began to show a

higher corrosion loss than the rest of the steels. The jump in the corrosion rate for T steel at week

57

70 is reflected in the total corrosion loss by an increased slope for the curve representing this steel. After 70 weeks of testing, CRPT1 showed the lowest total corrosion loss with values of 4.34 μm, followed by CRT with 5.20 μm, T steel with 5.75 μm, and N steel with 5.79 μm. CRPT2 steel had the highest total corrosion loss with 6.50 μm.
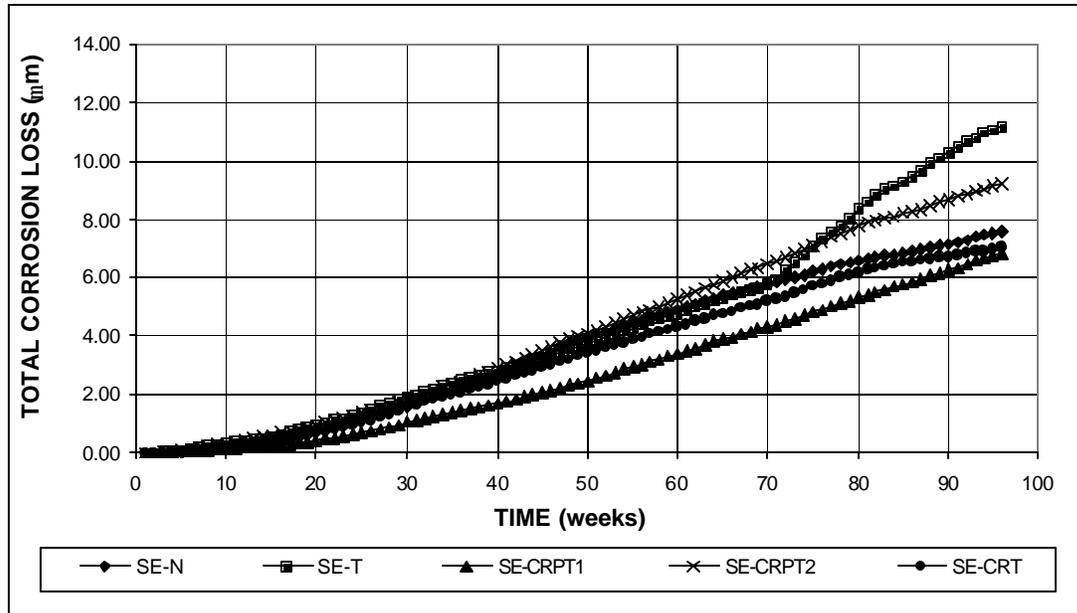
Figure 3.11: Southern Exposure Test – Average Total Corrosion Loss

Figure 3.12 shows the total corrosion loss for specimens with mixed steels. Figures A.49 to A.53 show the results for the individual specimens. The corrosion rates are very similar for both types of specimens throughout the testing period and no difference in corrosion loss is observed between the average plots until week 65 when the specimens with CRPT1 steel on the top mat started to show a slightly higher average corrosion loss. After 70 weeks of testing, specimens with N steel on the top mat had an average total corrosion loss of 6.08 μm and specimens with CRPT1 steel on the top mat had an average total corrosion loss of 6.51 μm.
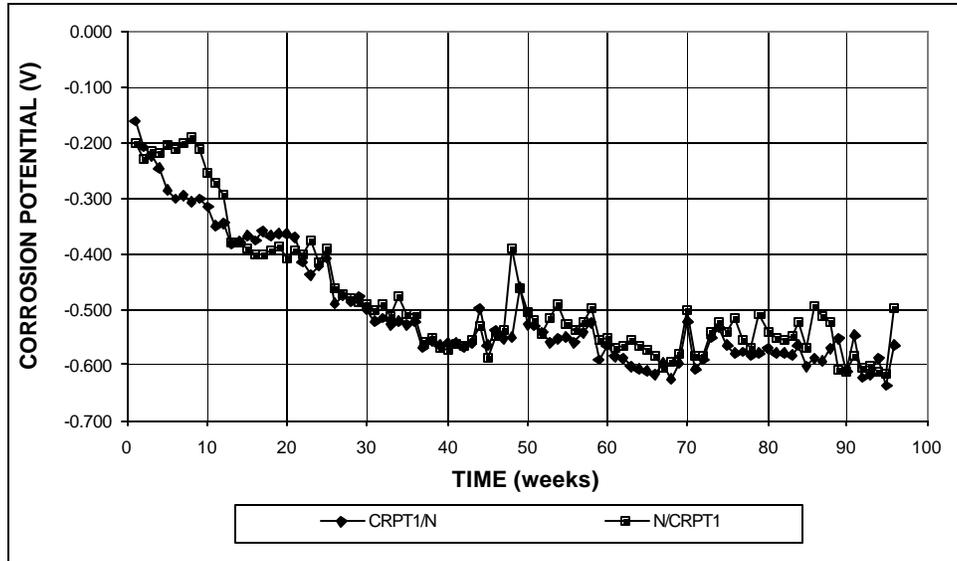
FIGURE 3.12: Southern Exposure Test – Average Total Corrosion Loss, Specimens with Mixed Steel

Figures 3.13 and 3.14 show the average corrosion potentials versus a copper-copper sulfate electrode for the top mat of steel. Figures A.56 to A.62 show the results for the individual specimens. After the first week, the corrosion potential of the top mat for all steels was above –0.250 V but decreasing fairly rapidly. By week 6 the corrosion potential of all steels was below –0.350 V, with the exception of CRPT1, which did not fall below this value until week 16. A potential more negative than –0.350 V versus the copper-copper sulfate electrode indicates that the steel has begun to corrode. CRPT1 showed a more positive corrosion potential than the other steels for the first 35 weeks, after which all steels had a similar potential. The potential of the top mat decreased with time for all steels. From week 40 until the end of the testing period, the corrosion potential for all steels has between –0.500 and –0.600 V, which indicates that there is a high probability that corrosion has occurring. Specimens with mixed steel showed a similar behavior. The corrosion potential of the top mat started at approximately –0.200 V and began

59

decreasing with time. At week 12 it had a corrosion potential of approximately –0.350 V, which indicates a loss of passivity. By week 40 the corrosion potential had reached values between –0.500 and –0.600 V and remain relatively constant for the rest of the testing period.
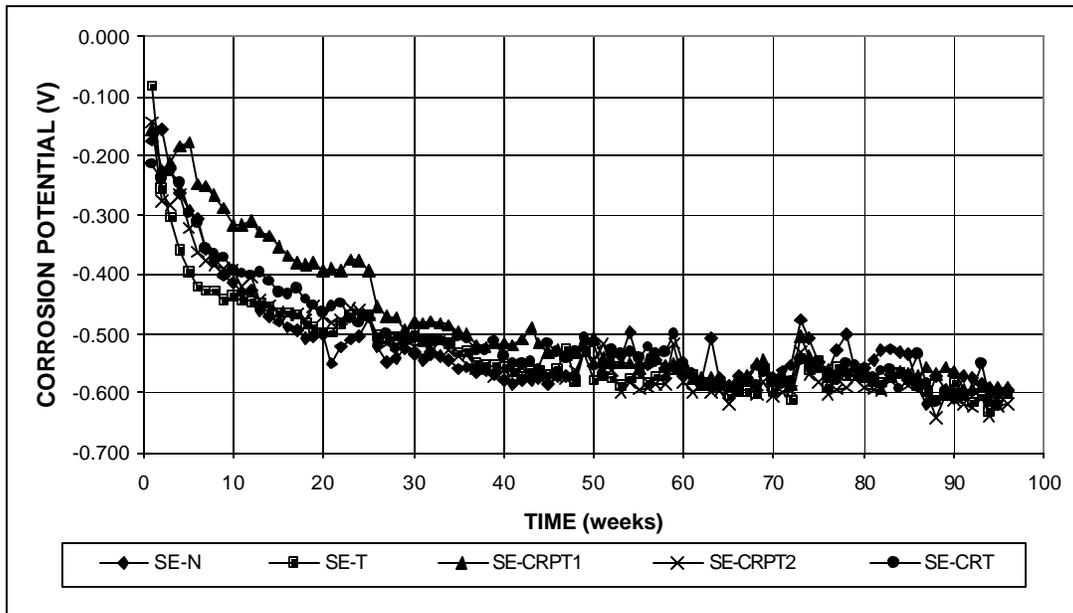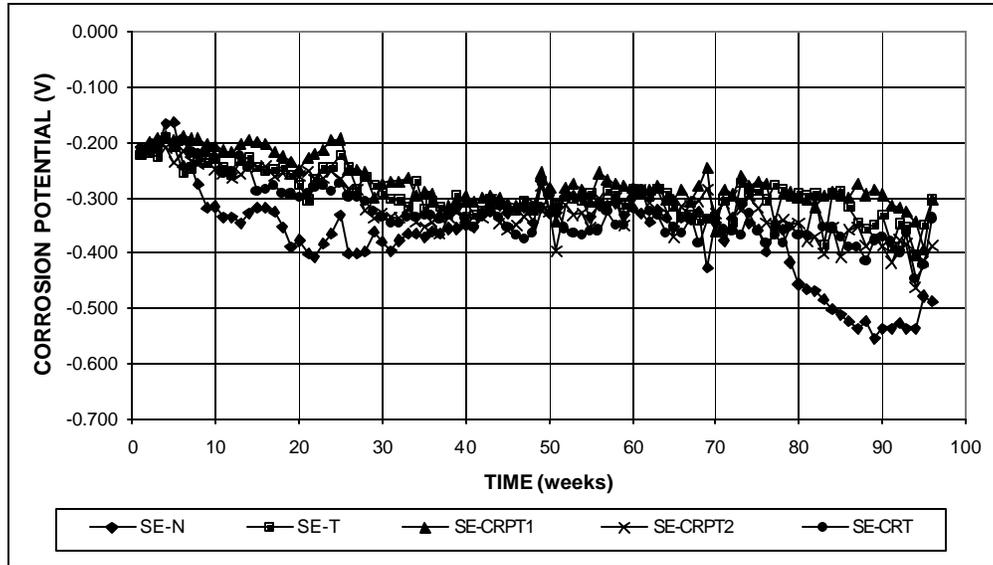

FIGURE 3.13: Southern Exposure Test – Average Corrosion Potential versus Copper-Copper Sulfate Electrode, Top Mat
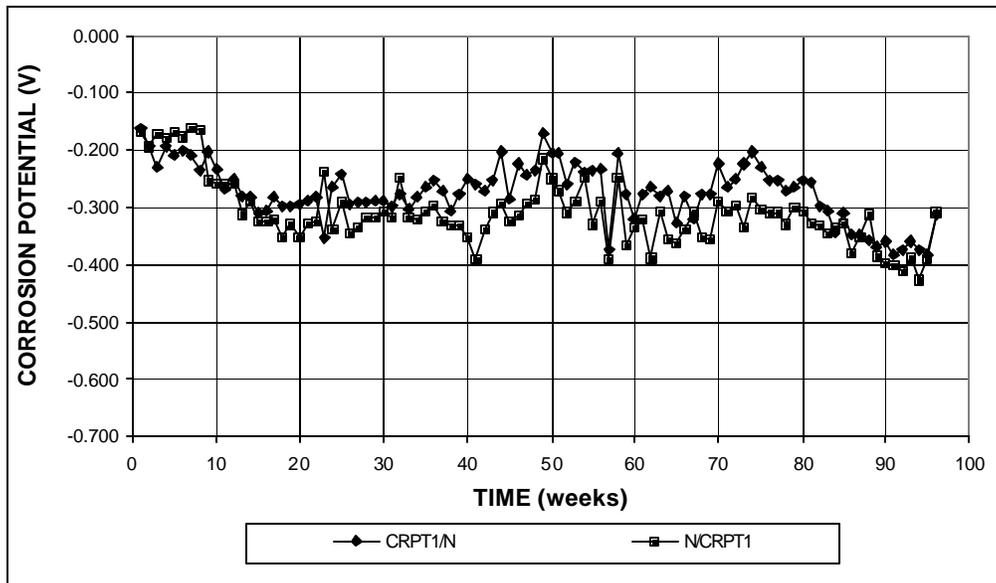
FIGURE 3.14: Southern Exposure Test – Average Corrosion Potential versus Copper-Copper Sulfate Electrode, Top Mat (Specimens with Mixed Steel)

Figures 3.15 and 3.16 show the average corrosion potentials versus the copper-copper sulfate electrode for the bottom mat of steel. Figures A.63 to A.69 show the results for the individual specimens. During the first week the average potential for all steels has approximately –0.200 V, then started to decrease slightly until it reaches values between –0.300 and –0.375 V after 35 weeks, which indicates that it is uncertain if the steel is corroding. The potentials remain in this range until week 70 when some steels exhibited a potential close to –0.400 V. This drop in potential indicates a high probability that chlorides had reached the bottom mat of steel. At week 79, the corrosion potential of N steel dropped and reached values close to –0.550 V at week 90. For the specimens with mixed steel, the corrosion potential of the bottom mat has approximately –0.200 V for the first 9 weeks, after which it dropped to –0.300 V until week 80. Up to this point the steel in the bottom mat is passive. After week 80 the corrosion potential of the top mat became more negative, and by week 90, the potential is –0.400V, which indicates a high probability that chlorides have reached the bottom mat of steel.

61

FIGURE 3.15: Southern Exposure Test – Average Corrosion Potential versus Copper-Copper Sulfate Electrode, Bottom Mat

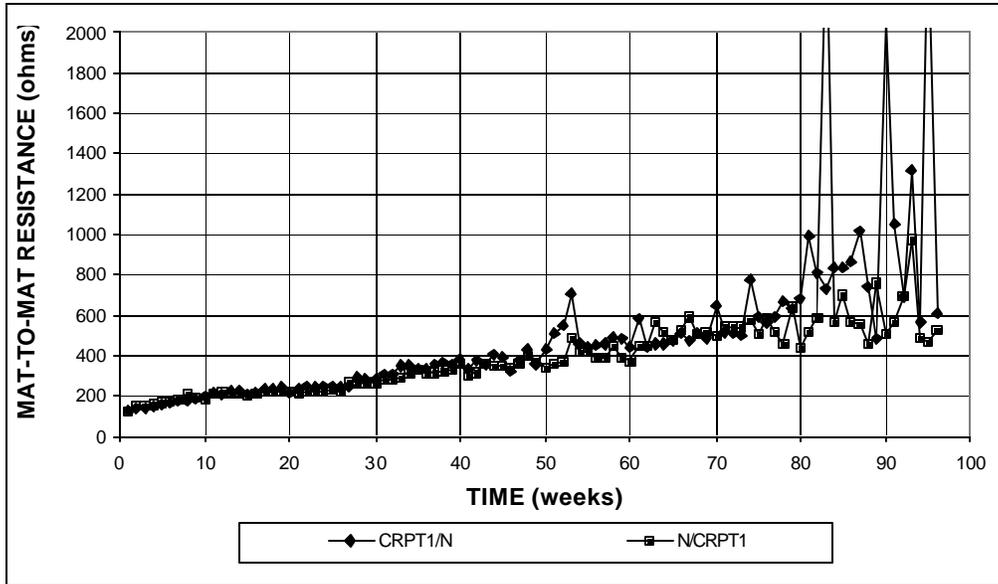**FIGURE 3.16: Southern Exposure Test – Average Corrosion Potential versus Copper-Copper Sulfate Electrode, Bottom Mat (Specimens with mixed steel)**

Figures 3.17 and 3.18 show the average mat-to-mat resistance. Figures A.70 to A.76 show the results for the individual specimens. The average mat-to-mat resistance for weeks 1 and 70 of the testing period are given in Tables 3.5 and 3.6, respectively. The mat-to-mat resistances

for all steels started close to 150 ohms and increase with time. Up to week 50 all steels showed

very similar mat-to-mat resistance, with very little scatter. After this period, the average plots

showed more scatter, but in general, the values continued to increases with time. Mat-to-mat

resistance for N steel showed a drop in value after week 80, indicating the possible formation of

cracks in the specimens. The average mat-to-mat resistances at week 70 show that N and

CRPT2 had the lowest mat-to-mat resistance, with 908 and 973 ohms, respectively. The highest

mat-to-mat resistances at this point were for T steel with 1678 ohms and CRPT1 steel with 1801

ohms. CRT steel had a mat-to-mat resistance at week 70 of 1048 ohms. Specimens with mixed

steels started with mat-to-mat resistances of approximately 130 ohms, and at week 70 they

showed values of 652 and 419 ohms.
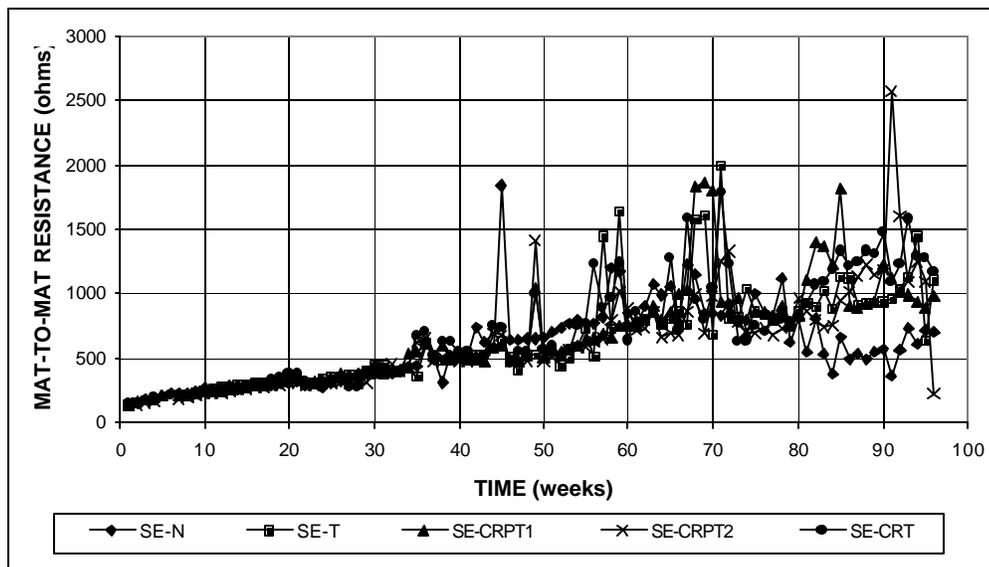
**FIGURE 3.17: Southern Exposure Test – Average Mat-to-Mat Resistance**

FIGURE 3.18: Southern Exposure Test – Average Mat-to-Mat Resistance, Specimens with Mixed Steel

3.2.2   Cracked Beam Test

As shown in Table 3.3, at week 70, CRPT2 and CRT had the lowest average corrosion rates (4.08 µm/year for CRPT2 and 4.17 µm/year for CRT), and N steel had the highest average corrosion rate with 7.34 µm/year. CRPT1 and T steels had intermediate values of corrosion rate. Average corrosion losses (Table 3.4) show that at week 70, CRT had the lowest corrosion loss with 7.24 µm, 4% less than conventional steel, which had a corrosion loss of 7.51 µm. T steel had the highest corrosion loss with 8.72 µm. CRPT1 and CRPT2 had corrosion losses of 7.50 and 8.17 µm, respectively. The mat-to-mat resistances after one week ranged from 246 to 325 ohms, and by week 70, the values were between 1986 and 2375 ohms. The values obtained in the CB test are higher than those observed in the SE test. This is attributed to the fact that the chlorides reached the top mat of steel on the CB specimen on the first day of testing and deposition of corrosion products started earlier. Corrosion potentials for the top mat at week 70 ranged from –0.579 to –0.630 V, which indicates that the steel was actively corroding. The bottom mat has corrosion potentials that ranged from –0.252 to –0.505 V. As discussed before, values more negative than –0.350 V indicate a high tendency to corrode. This occurred for the

bottom mat of steel once chlorides reached that level. Corrosion potential values that are more positive than –0.350 V indicate that the steel is passive.
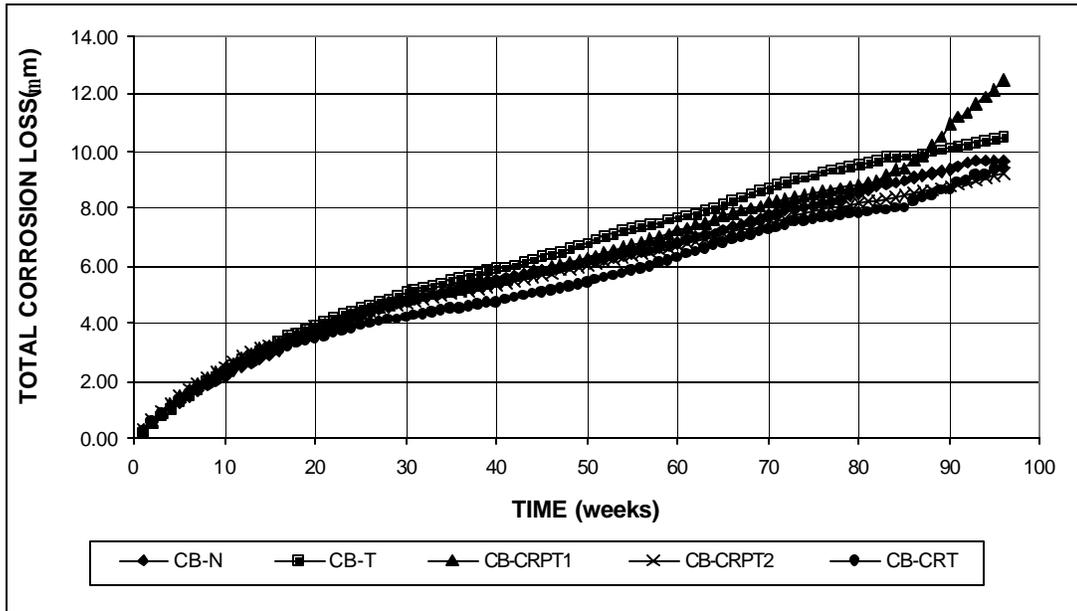
Average corrosion rates for the cracked beam specimens are shown in Figure 3.19, and the average corrosion rates for week 70 of testing are summarized in Table 3.4. Figures A.77 to A.81 show the results for the individual specimens. Since the crack allowed for direct access of the salt solution to the bars, the average corrosion rates during the first week showed values above 15 μm/year. The corrosion rates decreased with time and by week 30, all steels showed values below 5 μm/year. After week 80, CRPT1 and CRT started showing increased corrosion rates.
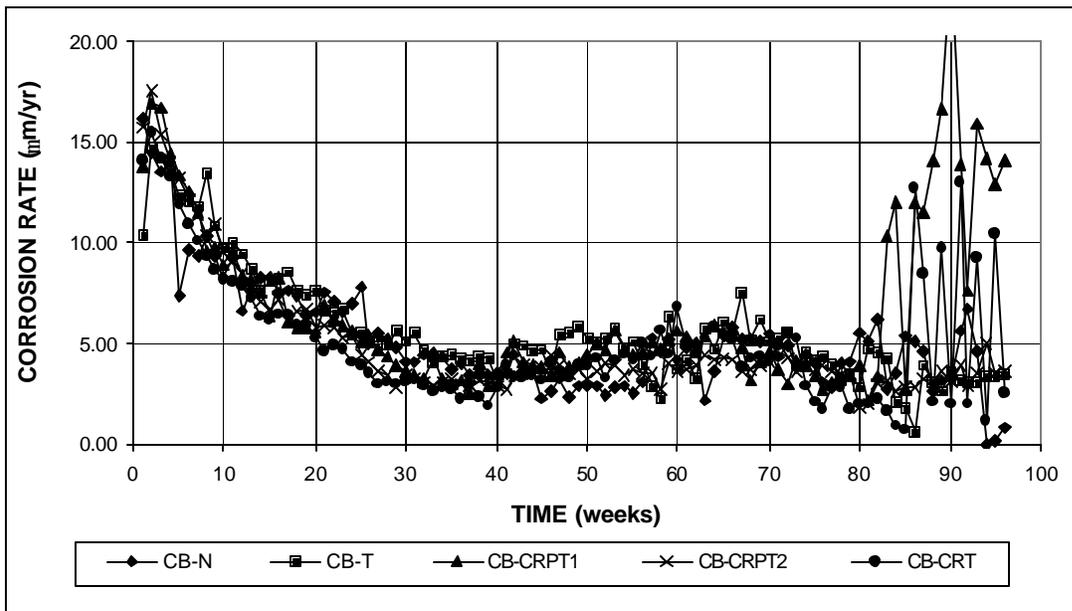
FIGURE 3.19: Cracked Beam Test – Average Corrosion Rate

The average total corrosion loss, shown in Figure 3.20, was similar for all steels. After week 30, CRT showed a lower value than the rest of the steels and this was maintained through week 90, when CRPT2 showed the lowest total corrosion loss. After week 40, T steel showed a higher value than the rest of the steels. After week 85, the curve representing CRPT1 steel showed a sharp increase in its slope. By the end of week 70 CRT steel had the lowest corrosion

loss with 7.25 μm followed by CRPT2 with 7.49 μm and N steel with 7.75 μm. The highest

corrosion losses were for T steel with 8.81 μm and CRPT1 steel with 8.73 μm. Figures A.82 to

A.86 show the plots for the individual specimens.

FIGURE 3.20: Cracked Beam Test – Average Total Corrosion Loss

Figure 3.21 shows the average corrosion potentials versus the saturated calomel electrode

for the top mat of steel. Figures A.87 to A.91 show the results for the individual specimens.

Starting in the first week, all corrosion potentials for the top mat were well below –0.500 V, and

all steels showed similar values, indicating that all had a similar tendency to corrode.

Throughout the testing period, the corrosion potential ranged from –0.500 V to –0.650 V, and

there is no difference between the steels.

66
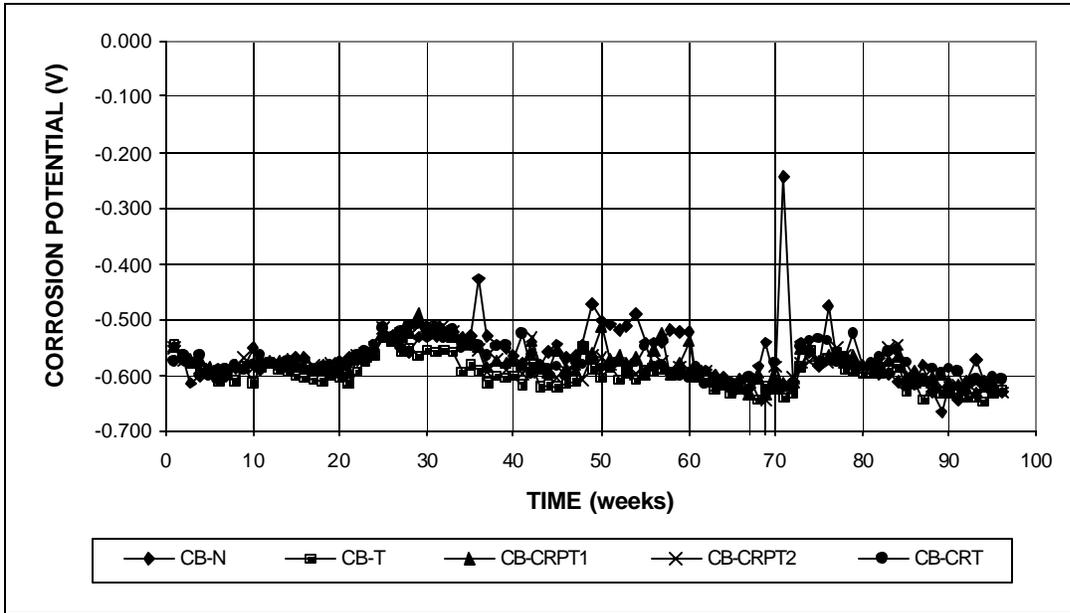
FIGURE 3.21: Cracked Beam Test – Average Corrosion Potential versus Copper-Copper Sulfate Electrode, Top Mat

Figure 3.22 shows the average corrosion potentials versus the saturated calomel electrode for the bottom mat of steel. Figures A.92 to A.96 show the results for the individual specimens. After 1 week of testing all steels had a bottom mat corrosion potential between –0.200 and –0.250 V, which indicates a passive condition. The corrosion potential remained above –0.350 V until week 60 for all steels, with the exception of N steel, which showed values close to –0.400 V from week 11 to week 30. After week 60, all specimens showed a slight decrease in the corrosion potential of the bottom mat, which might indicate the presence of chloride ions at the level of this barst. N steel showed the most negative corrosion potential, and by week 90 it reached values lower than –0.500 V. CRPT2 steel showed the most positive corrosion potentials during the last weeks of testing.

67
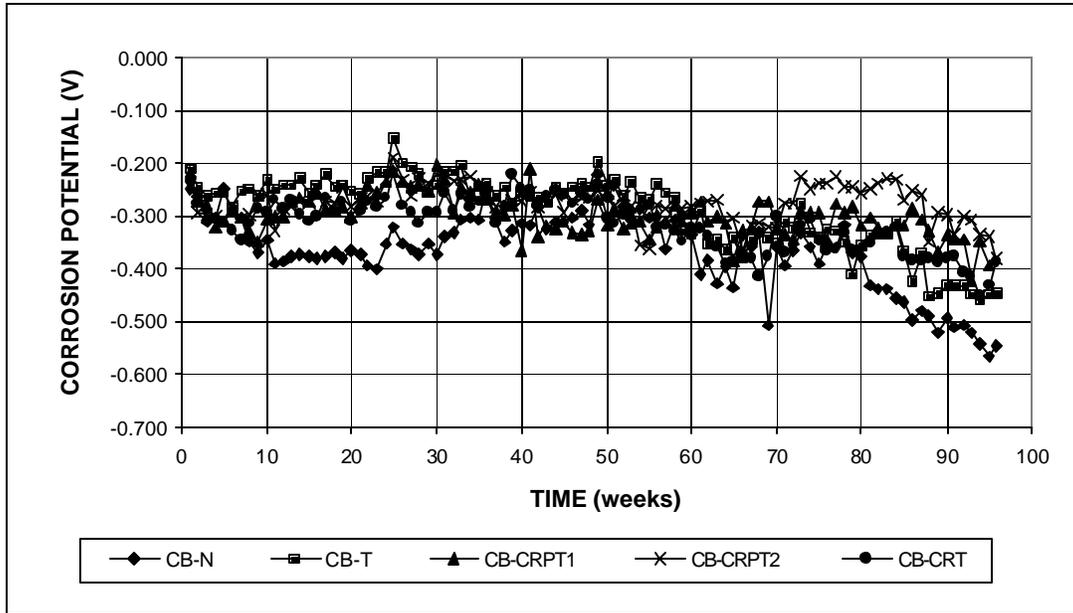
FIGURE 3.22: Cracked Beam Test – Average Corrosion Potential versus Copper-Copper Sulfate Electrode, Bottom Mat

Figure 3.23 shows the average mat-to-mat resistance. Figures A.97 to A.101 show the results for the individual specimens. The average mat-to-mat resistance for the first week of testing is given in Table 3.5. All steels started with values of mat-to-mat resistance close to 300 ohms and increaseed with time. As in the SE tests, up to week 50 all steels showed very similar mat-to-mat resistance, and very little scatter. After this period the average plot showed more scatter, but in general, the values continued to increases with time. Similarly to the SE test, N steel showed a drop in the average mat-to-mat resistance after week 80. The average mat-to-mat resistance for week 70 is given in Table 3.6. These values show that CRT steel had the lowest mat-to-mat resistance, 1986 ohms, followed by CRPT1 steel with 2005 ohms, and T steel with 2087 ohms. The highest mat-to-mat resistances at the end of the testing period were for CRPT2 steel with 2375 ohms and N steel with 3603 ohms.
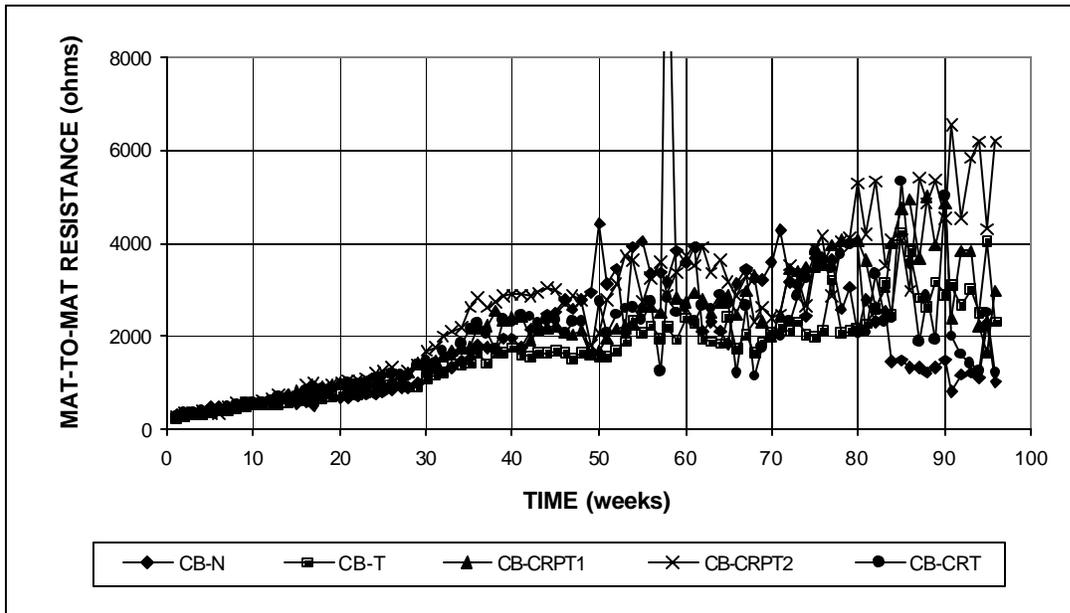
FIGURE 3.23: Cracked Beam Test – Average Mat-to-Mat Resistance

3.2.3   ASTM G 109 Test

As shown in Table 3.3, at week 70, T and CRT steels had the lowest average corrosion rates (2.85 µm/year for T steel and 3.01 µm/year for CRT), while N and CRPT1 steel had the highest corrosion rate (3.80 µm/year for N steel and 3.92 µm/year for CRPT1 steel). CRPT2 steel had a corrosion rate of 3.40 µm/year. The average total corrosion loss shown in Table 3.4 indicates that after 70 weeks CRT had the least corrosion loss with 0.94 µm, only 36 percent of the value for N steel, which had the highest corrosion loss with 2.61 µm. Mat-to-mat resistance for all specimens was between 159 and 212 ohms after 1 week, and increased to values between 906 and 1216 ohms by week 70. Average corrosion potential of the top mat for all steels ranged from –0.374 to –0.516 V, which indicates a high tendency to corrode. Average corrosion potential of the bottom mat ranged from –0.187 to –0.317 V, which indicates that chlorides had not reached the bottom mat of steel in some specimens.

Average corrosion rates for the G 109 specimens are shown in Figure 3.24, and the average corrosion rates at week 70 are summarized in Table 3.5. Figures A.102 to A.106 show the results for the individual specimens. Unlike the Southern Exposure and cracked beam tests, corrosion rates remained close to zero for several months after the tests have started. The first steel to show activity was N steel at week 18, followed by T and CRPT2 steels at week 22, CRPT1 steel at week 31 and CRT at week 39. Corrosion rates reached nearly constant values after week 60 for all steels and values ranged from 2 to 4 μm/year. N steel showed the lowest corrosion rates after week 70 with values between 1 and 2 μm/year. Once corrosion starts, the G 109 specimens exhibited large differences in corrosion rate from week to week. This variation was due to the four-week ponding and drying cycle used for these specimens.
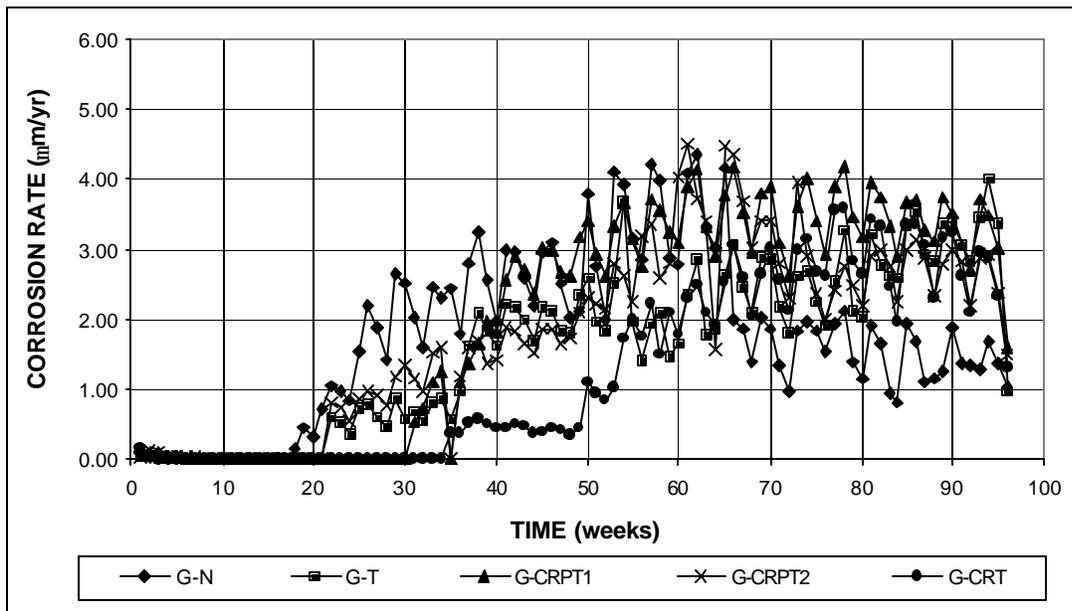
FIGURE 3.24: G 109 Test – Average Corrosion Rate

Total corrosion losses versus time are plotted in Figure 3.25, and values at week 70 are given in Table 3.4. Figures A.107 to A.111 show the results for the individual specimens. N steel shows the highest corrosion loss during the testing period as it started corroding earlier than

70

the other steels. CRT steel shows the lowest corrosion loss as it started corroding last, which might indicate a slightly higher corrosion threshold. The slopes for the five curves are very similar because the corrosion rates are similar once the steels start to corrode. N steel shows a change in slope at the end of the testing period since, as mentioned above, its corrosion rate dropped at the end of the testing period. This decrease coincided with a large increase in mat-to-mat resistance, indicating that the deposition of corrosion products was high enough to decrease the rate of corrosion, and not that the steel is more corrosion-resistant. After 70 weeks, CRT showed the lowest total corrosion loss with a value of 0.94 µm, followed by T steel with 1.61 µm, CRPT2 steel with 1.98 µm, and CRPT1 steel with 2.10 µm. N steel had the highest total corrosion loss with 2.46 µm.
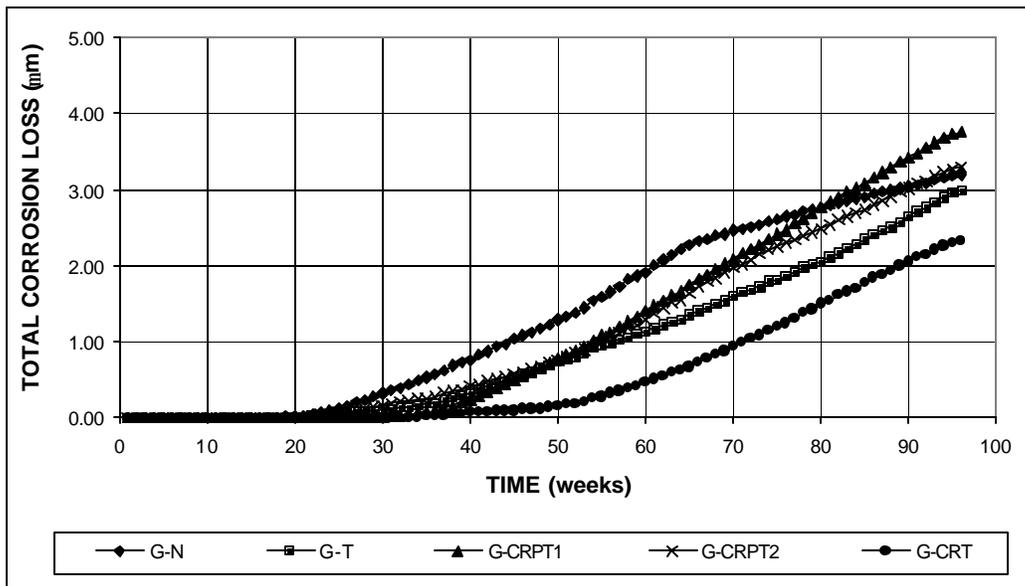
FIGURE 3.25: G 109 Test – Average Total Corrosion Loss

The average corrosion potentials versus a copper-copper sulfate electrode for the top and bottom mats of steel are shown in Figures 3.26 and 3.27. The results for the individual specimens are shown in Figures A.112 to A.121. The potential of the top mat of steel for all specimens was more positive than –0.200 V during the first 30 weeks of testing, with the exception of N steel,

71

for which the potential began to drop at week 21. By week 36 the potential of the top mat for N steel was below –0.500 V, while for the rest of the steels it was above –0.250 V. The potential for the rest of the steels began to drop at week 35 and reached values close to –0.400 V by week 60. The corrosion potential of the bottom mat had values above –0.200 V for all steels until week 60, except for N steel which had values below –0.200 V at week 30. During the last weeks of testing, all steels showed bottom mat corrosion potentials between –0.200 and –0.300 V.
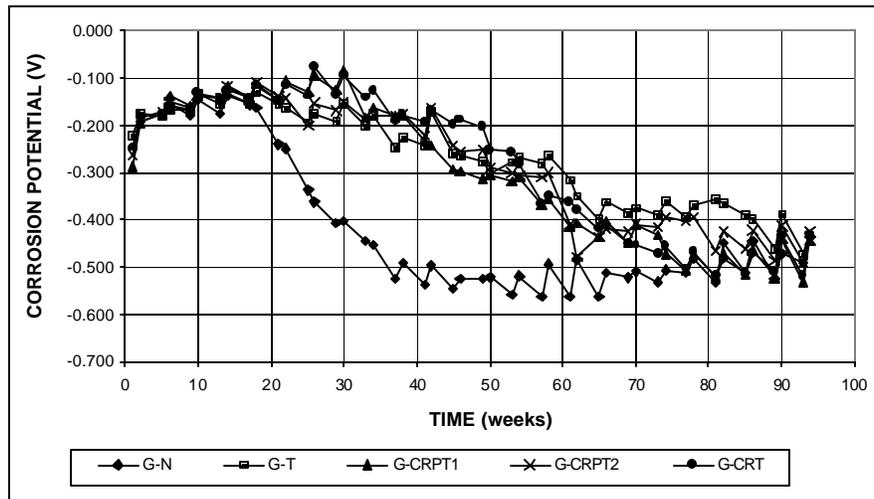
FIGURE 3.26: G 109 Test – Average Corrosion Potential versus Copper-Copper Sulfate Electrode (Top Mat)

FIGURE 3.26: G 109 Test – Average Corrosion Potential versus Copper-Copper Sulfate Electrode (Bottom Mat)

72
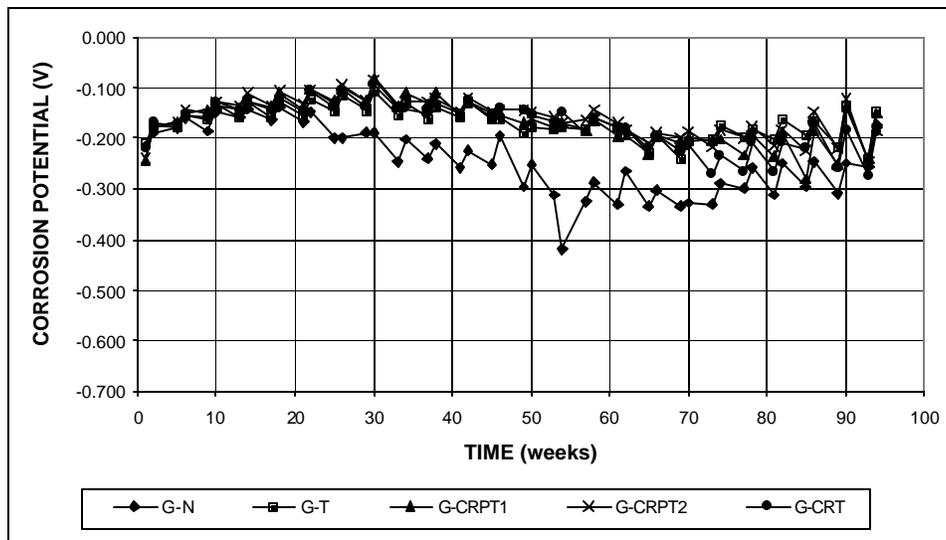
Figure 3.28 shows the average mat-to-mat resistance and Tables 3.5 and 3.6 give the average mat-to-mat resistance for weeks 1 and 70, respectively. Figures A.122 to A.126 show the results for the individual specimens. All steels starterd with values of mat-to-mat resistance between 150 and 220 ohms, which increased with time. Throughout most of the testing period, all steels showed similar mat-to-mat resistances. During the last weeks of testing the mat-to-mat resistance of N steel increased rapidly in comparison to the other steels. The average mat-to-mat resistance at week 70 is given in Table 3.5. These values show that CRPT1 steel had the lowest mat-to-mat resistance, 948 ohms, followed by CRT steel with 1116 ohms, and CRPT2 steel with 1126 ohms. The highest mat-to-mat resistances were for T steel with 1244 ohms and N steel with 1283 ohms.
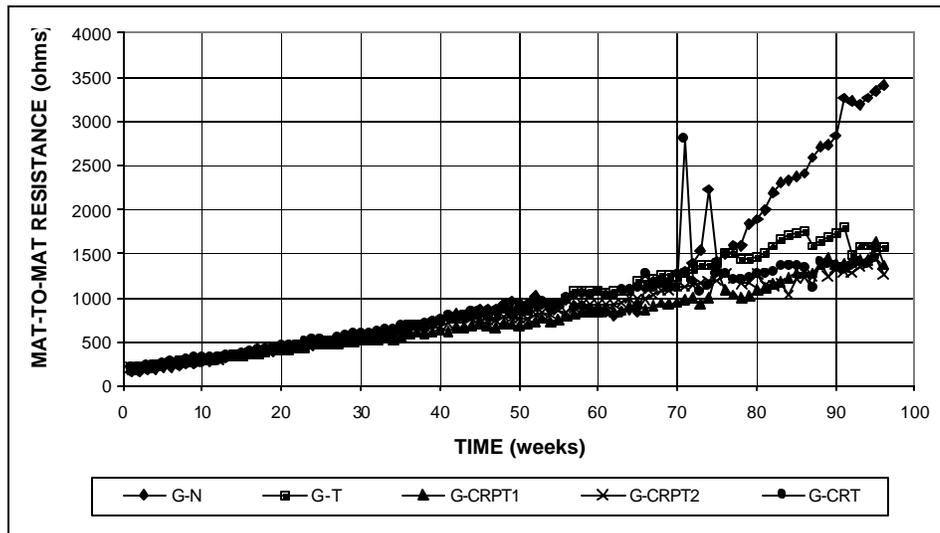
FIGURE 3.28: G 109 Test – Average Mat-to-Mat Resistance

3.2.4   Appearance of Specimens

After the 96-week test period, a visual inspection of the bars was performed. The concrete portions of the specimens were destroyed and the bars were removed and photographed. Figures 3.29 to 3.34 show representative pictures obtained from the specimens.

Rust stains were observed on the surface of some Southern Exposure specimens, as shown in Figure 3.29. The surface of the cracked beam specimens was completely stained because the corrosion products were carried to the surface of the specimen through the cracks. Very thin cracks that ran parallel to the reinforcing bars, as shown in Figure 3.30, were also observed on some of the Southern Exposure specimens. The G 109 specimens did not show cracks or rust stains on the concrete.

Figures 3.31 to 3.34 show the corrosion products observed on some of the specimens with different types of steel. Figures 3.31 and 3.32 show one of the top bars of specimens SE-N-3 and SE-CRPT2-1, respectively, and the corrosion products surrounding them, after the concrete cover was removed. Figure 3.33 shows a side view of one of the top bars of specimen SE-CRT-1. In the three cases shown, corrosion products were a combination of greenish-black and red-brown products. The greenish-black corrosion products are ferrous hydroxide, while the red-brown corrosion products are ferric oxides, which form when the ferrous hydroxides react with oxygen. The greenish-black products changed to a red-brown color after several hours. Figure 3.34 shows the bottom bars of specimen SE-CRPT1-3. Corrosion products were observed on the four bars. As shown in Figure A.60, the corrosion potential of the bottom bars had dropped below –0.350 V versus the copper-copper sulfate electrode, which indicated the high probability of corrosion on these bars.

FIGURE 3.29: Rust Stains on Surface of Specimen SE-CRPT2-1

FIGURE 3.30: Thin Cracks on Specimen SE-CRPT1/N-3

FIGURE 3.31: Corrosion Products on Top Bar of Specimen SE-N-3

FIGURE 3.32: Corrosion Products on Top Bar of Specimen SE-CRPT2-1

FIGURE 3.33: Corrosion Products on Top Bar of Specimen SE-CRT-1
(Side View of Specimen)

FIGURE 3.34: Corrosion Products on Bottom Bars of Specimen SE-CRPT1-3

3.3 Mechanical Tests

The mechanical properties of four steels, T, CRPT1, CRPT2, and CRT were tested according to ASTM A 615. The results are shown in Table 3.9. Stress-strain curves for each sample are shown in Figures A.126 to A.137. All steels met the requirements of ASTM A 615 for tensile strength, yield strength, and percent elongation for Grade 420 [Grade 60] steel. The results obtained for all steels were similar to those reported by Gerdau AmeriSteel (Table 2.2). All steels met the minimum bending requirements, which indicates that the higher alloy contents, especially phosphorus, did not affect the ductility of the steel. The results indicate that the microalloyed steels can be used as a replacement for standard A 615 reinforcement.

TABLE 3.9: Mechanical Tests

Steel Designation	Yield Strength		Tensile Strength		Elongation in 202.3 mm (8 in.)	Bending
	(MPa)	(ksi)	(MPa)	(ksi)		
T	561.3	81.4	715.0	103.7	14.8%	OK
	559.9	81.2	716.4	103.9	13.3%	OK
	573.7	83.2	727.4	105.5	12.5%	OK
	564.9	81.9	719.6	104.4	13.5%	OK
CRPT1	568.1	82.4	746.0	108.2	10.9%	OK
	591.6	85.8	746.0	108.2	10.9%	OK
	590.9	85.7	755.0	109.5	12.5%	OK
	583.5	84.6	749.0	108.6	11.4%	OK
CRPT2	577.8	83.8	775.7	112.5	13.3%	OK
	581.9	84.4	768.8	111.5	13.3%	OK
	579.2	84.0	770.9	111.8	14.1%	OK
	579.6	84.1	771.8	111.9	13.6%	OK
CRT	566.1	82.1	728.1	105.6	14.1%	OK
	517.1	75.0	727.4	105.5	12.5%	OK
	499.2	72.4	715.0	103.7	11.7%	OK
	527.5	76.5	723.5	104.9	12.8%	OK

3.4 Discussion

The corrosion potential test gives an indication of the tendency of a metal to corrode. As shown Section 3.1.1, the five steels had similar corrosion potentials when exposed to the same conditions. The steels were tested in a bare condition and with a mortar cover in NaCl and simulated concrete pore solution. On day 40 of the test, the least negative corrosion potential for

78

all the tests performed was –0.380 V, which indicates that the steels have a very high probability

of corrosion under those conditions. The corrosion potential test only gives the probability that

corrosion is occurring but does not indicate the rate of corrosion. The macrocell test allows the

corrosion rate of the bars to be measured when exposed to a NaCl and simulated concrete pore

solution. The bars were tested in a bare condition and embedded in mortar (Section 3.1.2). The

results for the different tests performed showed that the five steels had similar corrosion rates,

with no improved behavior for the microalloyed steels.

In the bench-scale tests, the corrosion rate, mat-to-mat resistance, and corrosion potential

of the top and bottom mats were used to monitor the specimens. One of the microalloyed steels,

CRT, showed consistently lower corrosion losses than conventional steel, after 70 weeks.

Although CRT appears to be much more corrosion resistant than conventional steel in the G 109

tests (64% less total corrosion loss after 70 weeks), its overall performance does not show such

an advantage. In the cracked beam test after 70 weeks, it had only 4 percent less corrosion loss

than conventional steel, which indicates that in cracked concrete the two steels behave in a

similar manner. In the Southern Exposure test, CRT steel had an 11 percent lower corrosion loss

than conventional steel after the same period. Comparison of the two conventional steels (N and

T) shows no advantage of the Thermex treated conventional steel (T) over the hot-rolled

conventional steel (N).

In all of the bench-scale tests, the mat-to-mat resistance increased with time due to the

deposition of corrosion products on the surface and in the region surrounding the reinforcing

bars. The corrosion potential of the top bars at week 70 was more negative than –0.350 V versus

a copper-copper sulfate electrode, indicating a high tendency to corrode, for all steels. The G 109

specimens exhibited less negative corrosion potentials than the other two tests. This behavior

results from the lower salt concentration at the level of the steel in the G 109 test, which is due to

the less aggressive ponding and drying cycles and the lower salt concentration used in the

ponding solution. The corrosion potential of the bottom mat of steel, at week 70, ranged from

–0.187 V to –0.420 V with respect to a copper-copper sulfate electrode. The values that were

more negative than -0.350 V indicate a high probability that the salt had reached the bottom

reinforcing bars.

All steels met the requirements of ASTM A 615 for tensile strength, yield strength, and

percent elongation for Grade 420 [Grade 60] steel as well as the minimum bending requirements,

which indicates that the higher alloy contents, especially phosphorus, did not affect the ductility

of the steel. The results indicate that the microalloyed steels can be used as a replacement for

standard A 615 reinforcement.

Chapter 4

Conclusions and Recommendations

4.1   Summary

The corrosion-resistant properties of three microalloyed and two conventional steels was performed. Earlier tests had shown that microalloyed steels similar to those in the study were twice as corrosion resistant as conventional steel. The same studies showed that, when epoxy-coated, the new steels were up to 10 times as corrosion resistant as conventional epoxy-coated steel. The microalloyed steels contained small amounts of chromium, copper and phosphorus that exceed the amounts allowed in ASTM specifications. One conventional steel and the three microalloyed steels were heat treated by the Thermex process, which included quenching and tempering of the steel immediately after rolling, and the other conventional steel was hot-rolled. The evaluation was performed using five different tests: the corrosion potential, corrosion macrocell, Southern Exposure, cracked beam, and ASTM G 109 tests. The tests used the corrosion potential and corrosion rate to evaluate the steel. Tension and bending tests were also performed to evaluate the effect of the microalloys and heat treatment on the mechanical properties of the reinforcing steel.

The five types of reinforcing steel tested, provided by Gerdau AmeriSteel, include: hot-rolled conventional steel (N); Thermex-treated conventional steel, (T); Thermex-treated microalloyed steel with a high phosphorus content, 0.117%, (CRPT1); Thermex-treated microalloyed steel with a high phosphorus content, 0.100%, (CRPT2); and Thermex-treated microalloyed steel with normal phosphorus content, 0.017%, (CRT).

Bars for the rapid evaluation tests were tested with and without mortar cover at two different NaCl ion concentrations (0.4 m and 1.6 m). A water-cement ratio of 0.5 and a sand-cement ratio of 2 were used for the mortar specimens. The bench-scale specimens had a water-cement ratio of 0.45. Specimens with a combination of conventional steel and microalloyed steel were also tested in the Southern Exposure test.

4.2   Conclusions

The following conclusions are based on the test results obtained in this study.

1.   The corrosion potential of the five steels was approximately the same, indicating that they have a similar tendency to corrode. By the last day of testing, the corrosion potential versus the saturated calomel electrode for all steels was more negative than –0.380 V, which indicates a high probability that corrosion was occurring.

2.   The corrosion rate of the five steels was approximately the same in the macrocell tests, indicating no improved corrosion protection for microalloyed steels over conventional steel.

3.   The microalloyed steel with regular phosphorus content (CRT) exhibited consistently lower corrosion losses than conventional steel on the bench-scale tests. This improved behavior, however, was not enough to use the steel without an epoxy coating or to justify continued research on the steel as a superior epoxy-coated material.

4.   The microalloying, including increased phosphorus, did not affect the mechanical properties or ductility of the steel. The mechanical properties of the microalloyed steel were similar to those of conventional steel.

5.   No improved corrosion performance was observed for the Thermex treated conventional steel over the hot-rolled conventional steel.

6.   The specimens with a combination of CRPT1 steel and conventional steel (N) had higher corrosion losses than specimens with only conventional steel.

7. The mat-to-mat resistance increased with time for all specimens, indicating the deposition of corrosion products on the surface and adjacent to the bars.

8. In the bench-scale tests, the corrosion potential versus the copper-copper sulfate electrode at week 70 for all steels was more negative than –0.374 V, indicating a high probability that corrosion was occurring.

9. In some bench-scale specimens the corrosion potential of the bottom mat became more negative during the last weeks of testing, indicating that chlorides had reached the bottom steel.

4.3   Recommendations

Based on the test results and conclusions presented in this report, it is recommended that microalloyed steel should not be used as part of a corrosion protection system. The three microalloyed steels showed no advantage over conventional steel in the macrocell tests, and the corrosion potential of the five steels evaluated was very similar, indicating that they have approximately the same tendency to corrode. CRT steel showed lower corrosion losses than N steel in the bench-scale tests, but the difference was only 11 percent in the Southern Exposure test and 4 percent in the Cracked Beam test, which is only a slight advantage over conventional steel in uncracked concrete and basically the same behavior as conventional steel in cracked concrete. The new steels did not duplicate the performance of earlier microalloyed steel that corroded at only 50 percent of the rate of conventional steel. Although CRT steel had only 36 percent the corrosion loss of conventional steel in the G 109 tests, its overall performance does not justify its use as uncoated steel or the pursuit of additional research on its use as epoxy-coated reinforcement.

REFERENCES

ASTM A 615/A 615M-00, (2001). "Standard Specification for Deformed and Plain Billet-Steel Bars for Concrete Reinforcement," *2001 Annual Book of ASTM Standards*, Vol. 03.01, American Society for Testing and Materials, West Conshohocken, PA.

ASTM C 150-00 (2002). "Standard Specification for Portland Cement," *2002 Annual Book of ASTM Standards*, Vol. 04.01, American Society for Testing and Materials, West Conshohocken, PA.

ASTM C 192/C 192M-00 (2002). "Practice for Making and Curing Concrete Test Specimens in the Laboratory," *2002 Annual Book of ASTM Standards*, Vol. 04.04, American Society for Testing and Materials, West Conshohocken, PA.

ASTM C 305-99, (2002). "Standard Practice for Mechanical Mixing of Hydraulic Cement Pastes and Mortars of Plastic Consistency," *2002 Annual Book of ASTM Standards*, Vol. 04.01, American Society for Testing and Materials, West Conshohocken, PA.

ASTM C 778-00, (2002). "Standard Specification for Standard Sand," *2002 Annual Book of ASTM Standards*, Vol. 04.01, American Society for Testing and Materials, West Conshohocken, PA.

ASTM C 876-91, (2002). "Standard Test Method for Half-Cell Potentials of Uncoated Reinforcing Steel in Concrete," *2002 Annual Book of ASTM Standards*, Vol. 03.02, American Society for Testing and Materials, West Conshohocken, PA.

ASTM G 109-99a (2002). "Standard Test Method for Determining the Effects of Chemical Admixtures on the Corrosion of Embedded Steel Reinforcement in Concrete Exposed to Chloride Environments," *2002 ASTM Annual Book of ASTM Standards*, Vol. 04.02, American Society for Testing and Materials, West Conshohocken, PA.

Darwin, D. (1995). "Corrosion-Resistant Reinforcing Steel," SL Report 95-2, University of Kansas Center for Research, Inc., Lawrence, KS, 22 pp.

Darwin, D., Locke, Browning, J.P, Nguyen, T.V., Carl E., Jr., (2002). "Mechanical and Corrosion Properties of a High-Strength, High Chromium Reinforcing Steel for Concrete". SM Report No. 66, University of Kansas Center for Research, Inc., Lawrence, KS, 142 pp.

Farzammehr, H., (1985). "Pore Solution Analysis of Sodium Chloride and Calcium Chloride Containing Cement Pastes," Master of Science Thesis, University of Oklahoma, Norman, OK.

Federal Highway Administration (FHWA) (1999), "1999 Status of the Nation's Highways, Bridges, and Transit: Conditions and Performance Report", FHWA website: http://www.fhwa.dot.gov/policy/1999cpr/index.htm.

Kahrs, J., Darwin, D., and Locke, Carl E., Jr., (2001). "Evaluation of Corrosion Resistance of Type 304 Stainless Steel Clad Reinforcing Bars," SM Report No. 65, University of Kansas Center for Research, Inc., Lawrence, KS, 76 pp.

Hausmann, D. A., (1965). "Steel Corrosion in Concrete", Materials Protection, Vol. 6, November 1967, pp. 19-23.

Jones, D.A. (1996). *Principles and Prevention of Corrosion*, Macmillan Publishing Company, New York, 572 pp.

Pfeifer, D. W., and Scali, M. J., (1981). "Concrete Sealers for Protection of Bridge Structures", National Cooperative Highway Research Board Program Report 244, Transportation Research Board, National Reseacrch Council, Washington, D.C., 138 pp.

Martinez, S. L., Darwin, D., McCabe, S. L., and Locke, Carl E., Jr., (1990). "Rapid Test for Corrosion Effects of Deicing Chemicals in Reinforced Concrete," SL Report 90-4, University of Kansas Center for Research, Inc., Lawrence, KS, 61 pp.

McDonald, D. B., Pfeifer, D. W., and Sherman, M. R., (1998). "Corrosion Evaluation of Epoxy-Coated, Metallic-Clad and Solid Metallic Reinforcing Bars in Concrete," Publication No. FHWA-RD-98-153, Federal Highway Administration, McLean, VA, 127 pp.

Nmai, C. K., Bury, Mark, A., and Farzam, H., (1994). "Corrosion evaluation of a sodium thiocyanate-based admixture," Concrete International: Design and Construction, v 16, n 4, Apr, 1994, p 22-25.

Senecal, M. R., Darwin, D., and Locke, Carl E., Jr., (1995). "Evaluation of Corrosion-Resistant Steel Reinforcing Bars," SM Report No. 40, University of Kansas Center for Research, Inc., Lawrence, KS, 142 pp.

Smith, J. L., Darwin, D., and Locke, C. E., Jr., (1995). "Corrosion-Resistant Steel Reinforcing Bars Initial Tests," SL Report 95-1, University of Kansas Center for Research, Inc., Lawrence, KS, 43 pp.

Schwensen, S. M., Darwin, D., and Locke, Carl E., Jr., (1995). "Rapid Evaluation of Corrosion-Resistant Concrete Reinforcing Steel in the Presence of Deicers," SL Report 95-6, University of Kansas Center for Research, Inc., Lawrence, KS, 90 pp.

Steinbach, O. F., and King, C. V. (1950). *Experiments in Physical Chemistry*, American Book Company, New York, 250 pp.

Tata Iron and Steel Co., (1991). "Development of New Corrosion Resistant Steel (CRS) Reinforcing Bars at Tata Steel," Report, Tata Iron and Steel Co., Jamshedpur, India, 32 pp.

Tourney, P., and Berke, N., (1993). "Call for standardized tests for corrosion inhibiting admixtures," Concrete International: Design and Construction, v 15, n 4, Apr. 1993, pp. 57-62.

Uhlig, Herbert H. and Revie, Winston R. (1985). *Corrosion and Corrosion Control. An Introduction to Corrosion Science and Engineering,* John Wiley & Sons, Inc., New York, 441 pp.